Recent Research Progress in Indophenine-Based-Functional Materials: Design, Synthesis, and Optoelectronic Applications

Shiwei Ren, Abderrahim Yassar

materials

MDPI

86 Review

Recent Research Progress in Indophenine-Based-Functional Materials: Design, Synthesis, and Optoelectronic Applications

Shiwei Ren[1], Abderrahim Yassar[2,*]

[1] Zhuhai Fudan Innovation Institution, Guangdong-Macao in-depth cooperation zone in Hengqin, 519000 P. R. China; shiwei_ren@fudan.edu.cn

[2] LPICM, Ecole Polytechnique, CNRS, Institut Polytechnique de Paris, Palaiseau, 91128 France ; abderrahim.yassar@polytechnique.edu

Abstract: This review highlights selected examples, from literatures from the last three-four years of the design, synthesis, properties, and device performance of quinoidal π-conjugated materials. A particular emphasis is placed on emerging materials, such as indophenine dyes that have the potential to enable high-performance devices. We specifically discuss the recent advances and design guidelines of π-conjugated quinoidal molecules from a chemical standpoint. To the best of the authors' knowledge, this review is the first compilation of the literature on indophenine-based semiconducting materials, their scope, limitations and applications. In the first section, we briefly introduce some of organic electronic devices which are the basic building blocks for certain applications involving organic semiconductors (OSCs). We introduce the definition of key performance parameters of three organic devices: organic field effect transistors (OFET), organic photovoltaics (OPV), and organic thermoelectric generators (TE). In section two, we review recent progress towards the synthesis of quinoidal semiconducting materials. Our focus will be on indophenine family that has never been reviewed. We discuss the structure/energy levels/properties relationship in this family of molecules. The last section reports the effect of structural modifications on the performance of devices: OFET, OPV and TE. By doing this, we have provided a general insight into the association between the molecular structure and electronic properties in quinoidal materials, in both small molecules and polymers. We also believe that the review offers benefits to the organic electronics and photovoltaic communities by reporting on recent trends in the synthesis and progression of promising novel building blocks that can provide guidance for synthesizing new generations of quinoidal or diradical materials with tunable optoelectronic properties and more outstanding charge carrier mobility.

Keywords: Quinoidal π-conjugated materials; OFETs; indophenine dyes

Citation: To be added by editorial staff during production.

Academic Editor: Firstname Lastname

Received: date
Revised: date
Accepted: date
Published: date

1. Introduction

Organic electronic devices have gained enormous popularity over the past 30 years because of their promising tunable electronic properties, flexibility, low-cost, versatile functionalization, and processability. The critical component of these devices is the OSC material, which serves as the active layer and determines the performance of the device. Over the last decade, one of the driving forces of development within this field is synthesizing novel high-performance building blocks and extending the library of organic materials for various optoelectronic and energy applications. Despite this the majority of work has been devoted to developing hole-transporting (p-type) OSCs, but less research has been done on electron-transporting (n-type) OSCs materials. One main reason for the lack of high-performance n-type OSCs is the availability of π-conjugated building units with strong electron-deficiency necessary to ensure sufficiently deep-lying LUMO energy and to enable the fabrication of n-type OSCs with stable electron transport features. For

electron transport materials, the majority can only undergo stable n-type transport when under conditions of nitrogen or vacuum, due to the fact that electron carriers can be easily trapped by H_2O and O_2 in the environment in the process of the device. It is generally assumed that a LUMO energy level at –4.0 eV is a prerequisite to developing a stable electron transport OSC, as the presence of a high electron affinity to facilitate electron injection and environmental stability facilitates the acquisition of high-performance electron transport OFETs. Along with this, the specific building blocks should have selective reaction sites that provide handles for insertion into the π-conjugated system and be readily compatible with a broad range of chemical reactions [1]. Frontier molecular orbital (FMO) energy levels (both HOMO and LUMO energy levels) can be accurately regulate by modification of the chemical structure to match the work function of the electrode. Despite the impressive work on the synthesis of n-type OSCs, the further development of novel building blocks enabling the production of high-performance materials remains a serious challenge. The exploration in this area has been driven by the development of new applications that require specific molecular design, namely non-fullerene organic solar cells, organic thin film transistors (OTFT), organic electrochemical transistors (OECT), organic thermoelectric (TE) generators, etc.

According to all databases from Web of Science, accessed in the winter of 2022, the number of published works in the domain of n-type and OSCs from 2004 to 2022 has exponentially increased, indicating the importance and interest of such emerging fields. There are one hundred review articles published related to n-type OSCs, synthesis design, characterization, and device function. Indophenine dyes are a sub-family of quinoidal small molecules having an oxindole moiety as a terminal group. According to SciFinder, there are only 106 scientific publications related to the indophenine molecules and no review article published in the open literature.

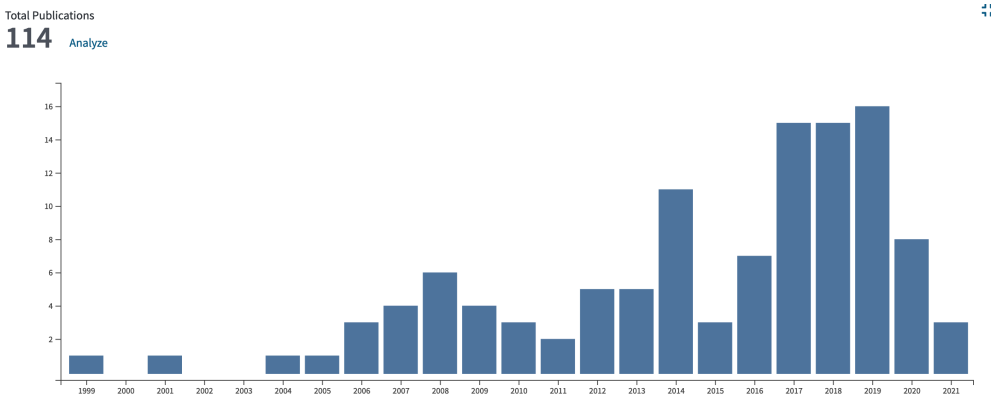

Figure 1. The number of review on the topic n-type OSCs from Thomson Reuters Web of Science: 114, of which the number of Quinoidal OSCs reviews: 9. Of the indophenine 106 references no reviews article reported according to Scifinder.

This review particularly highlights the recent advances in the emerging field of OSCs based on indophenine π-conjugated molecules, with particular emphasis on synthesis, characterization, device fabrication and function. By doing this, we aim to better define the relationship between the molecular structure (types and nature of building blocks, crystallinity, morphology, etc.) and the energies levels, air stability, together with charge carrier mobilities of devices. There are some reviews on n-type OSCs and quinoidal π-conjugated systems for optoelectronic and energy applications, but most of them cover only specific applications, and none of them the whole range from the molecular design, synthetic tactics to device performance.

2. Basic background of organic electronic devices and assessment parameters

In this section, we briefly outline certain organic electronic devices, which are the primary building blocks for various OSC-based applications. For a more detailed discussion, readers are referred to excellent reviews focusing on this topic [2,3,4,5,6,7].

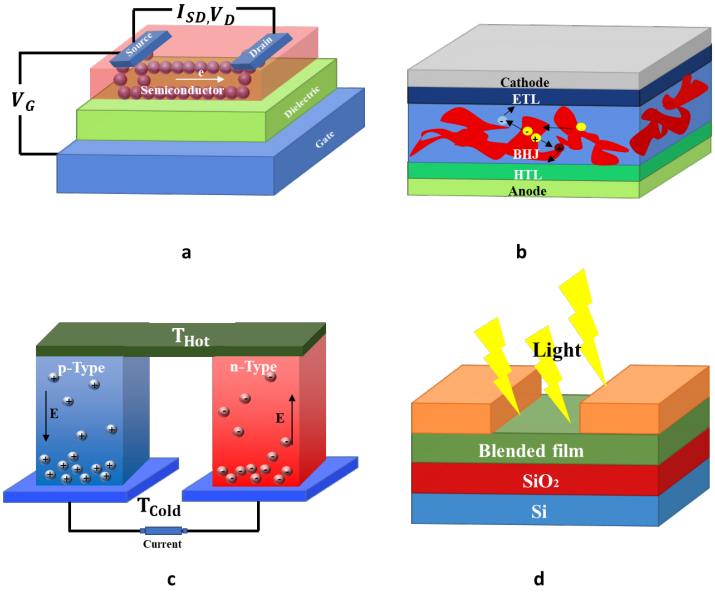

Figure 2. Representative thin-film optoelectronic devices that use OSC including: (a) a bottom-gate top-contact OFET; (b) a bulk heterojunction organic solar cell; (c) an organic TE device; (d) and a photo transistor.

OFETs are not only the fundamental building blocks of flexible and large area electronic devices, but are also a useful tool for measuring charge-carrier mobilities of newly OSCs and understanding, assessing charge transport behavior of OSCs. OFETs can be fabricated in different ways, with the most common constructions being the bottom-gate bottom-contact (BGBC) & bottom-gate top-contact (BGTC) structures [5]. For the first case, the source/drain electrodes are placed directly on the dielectric film, where most of the charge carriers are expected to be transported; whereas for the second case, the source & drain electrodes are positioned on top of the semiconducting layer and the charge carriers require crossing the semiconducting layer to arrive at the channel. Therefore, with those straightforward differences it means that the device configuration is able to affect the extracted charge mobility [4]. The OFETs can operate in two regimes: linear and saturation regimes. One figure of merit for OFETs is the charge mobility, which could be extracted by using OFET-equation in linear and/or saturation regimes. Although OFETs were already widely used to evaluate the charge transport characteristics in newly synthetized OSCs, nonetheless, it is challenging to compare charge transport parameters of different materials as the OFET-mobility is governed by several factors such as, the OFET-configuration used, the contact resistances, the choice of dielectric through its surface morphology and the morphology of active layer, etc.

The TE effect is a straight conversion of temperature differences into electric voltages and vice versa. Research attention is focused on novel TE-materials due to increasing energy demand and pollution linked to human activities. It should be remarked that approximately two-thirds of all industrial energy consumption is lost in the form of waste heat [8]. Consequently, it becomes urgent to promote the recovery of this huge waste heat into electrical energy. During the previous ten years, the number of teams active in the research of organic-TE materials has increased strongly. Since they are lightweight, printable and suitable for large area applications both p- and n-type TE materials become necessary in

practical applications. Yet, the efficiency of the TE is quite low. The performance of TE is commonly expressed in terms of TE figure of merit, $ZT = \sigma S^2 T/k$, whereby σ, S, T, and k respectively represent electrical conductivity, Seebeck coefficient, absolute temperature and thermal conductivity. [9]. The optimal TE-material should have either higher Seebeck coefficient for improved energy conversion, higher electrical conductivity for decreased joule heating, or lower thermal conductivity so as to conserve the temperature gradient. One of the challenges in the field of TE is the strong interdependence between the σ, S and κ, with optimization of any one of them causing a negative impact on at least one of the others.

Besides OFET and TE applications, n-type OSCs have also attracted considerable interest as alternative acceptors for non-fullerene solar cells[10] and electron-transporting materials for p-i-n perovskite. Organic and perovskite solar cells offer many benefits: flexibility, printability, low weight, low cost, fashionable designs and can be manufactured by roll-to-roll production, etc. For both types of solar cells, fullerenes and their derivatives have been broadly applied as acceptor for OPV. However, they suffer from a number of drawbacks such as weak light absorption in the visible-near infrared region, high-cost efficiency, etc. To address those limitations, OSCs have been extended to non-fullerene acceptor materials.

The past decade has witnessed tremendous development in molecular design guidelines for the discovery and synthesis of novel quinoidal π-conjugated materials. End-capped quinoidal π-conjugated molecules are a subfamily, with π-extended core having two terminal groups. They possess high electron acceptability and low LUMO levels, which has made them excellent n-type semiconductor materials, with electron mobilities well in excess of 1 $cm^2 V^{-1} s^{-1}$. The nature of π-extended core and terminal group have a profound effect on the electrical and optoelectronic properties in those materials.

In more detail below, we highlight selected examples from literatures from the last three-four years of the design, synthesis, properties, and device performance of quinoidal π-conjugated materials, with special attention to emerging materials like indophenine derivatives with promising potential for high performance devices. While there has been several outstanding reviews that have addressed the use of quinoidal oligothiophene as n-channel materials in OFETs[11], antiaromaticity and quinoid strategy as a tool for the design and synthesis of high-performance OFET materials[12], the role of the aromatic/quinoidal balance in determining the ground state of the quinoidal materials[13], understanding the structural evolution of quinoidal conjugated polymers for employed for electronics application, emphasizing the architecture of quinoidal frameworks and their attractive electronic structures[14].

In comparison the present work investigates the recent improvements and design guidelines for quinoidal molecules with a chemical perspective. To the authors' knowledge, this review represents one of the first compilation of the literature on the indophenine-based materials, their scope, progress, limitations, applications and prospects. We also consider this review to be benefit to the organic electronics and photovoltaic communities by reporting the latest trends of new building blocks which are available as high-performance materials. In the next section, we provide a review of state-of-the-art work in quinoidal semiconducting. Our main focus will be on indophenine series that has never been reviewed. We discuss the structure/energy levels/properties relationship in this family of molecules.

3. Synthetic tactics of π-extended quinoidal acceptors

π-Conjugated quinoidal molecules are emerging materials for energy and optoelectronic applications. Two main strategies have been developed by chemists for their synthesis. These approaches lead to two different classes of quinoidal materials. The first approach involves embedding the quinoidal moiety into the core of an aromatic π-conjugation. The second approach, known as end-group functionalization, involves terminal capping of the terminal methylene sites by electron-withdrawing functional group (EWG).

The functional groups, either cyano, ester groups or aryl groups, contribute to quinoidal character by blocking the reaction sites and delocalizing the spin. A π-extended core and terminal group have a profound effect on the electrical and optoelectronic performance of the resulting material. In the following section, it is briefly mentioned the general approach to the synthesis of quinoidal families with various terminal units. Four structural modification tactics are discussed in detail, involving the introduction of the dicyanomethylene functionality at the terminal positions of a π-conjugated system, indandione-terminated and triphenylmethane π-conjugated quinoids, and finally indophenine family. Generally, there are two main synthesis routes for the preparation of end-capped π-conjugated quinoidal molecules according to the reactivity and the functionality of the end-group. For quinoidal dicyanomethylene-end capped molecules, the Takahashi reaction is the most efficient way for their synthesis. In this route, the dibrominated aromatic compounds allow for a Takahashi coupling and then an oxidative dehydrogenation reaction to obtain the desired quinoidal forms (Route A, Figure 3). A quinoidal skeleton with four aryl groups bridged to it (Thiele's hydrocarbon) accessible by lithium-halogen exchange, followed by nucleophilic addition and reduction (route B). In the following, the rationale behind the design of these molecules and the methodology developed for their synthesis will be discussed based on the different precursors of forming quinoidal forms. In addition to the above routes, new methods have been reported, such as intra- or intermolecular radical–radical coupling reaction[15,16].

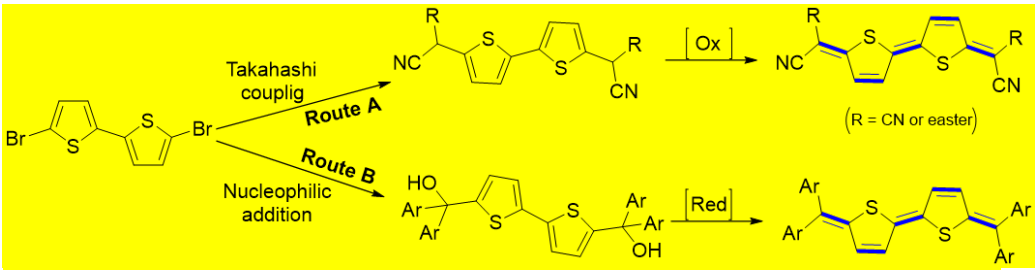

Figure 3. Typical synthetic strategies for the preparation of quinoidal π-conjugated molecules.

3.1. Recent advances of dicyanomethylene end-capped π-conjugated small molecules

Dicyanomethylene block is one of the moieties extensively involved in the construction of superior electron acceptor dyes. Its strong accepting ability arises from the vinyl extension of the conjugation length which promotes the planarity of the molecule and tends to achieve materials with improved charge carrier mobilities. The first synthesis of TCNQ (Figures 4) was published in the 1960s [17], since then various TCNQ derivatives have been reported [18,19]. This first synthesis was accomplished using a Knoevenagel condensation method, then oxidation using bromine[17]. To further improve the yield and simplify the reaction procedure, a new synthetic method has been developed by Takahashi and coworkers[20,21]. Since then, this reaction known as the Takahashi reaction has been widely used for preparing dicyanomethylene end-capped quinoidal molecules. In this reaction, the dihalogenated aromatics were converted into their respective quinoidal forms by a palladium-catalyzed coupling and followed by oxidation using Br_2 or 2,3-dichloro-5,6-dicyano-1,4-benzoquinone (DDQ) [22,23]. We recommend to our reader numerous review articles dedicated to covering TCNQ and its acceptor analogues from the point of view of design and synthesis[24], molecular architecture for optoelectronic applications[25], and optoelectronic devices[26].

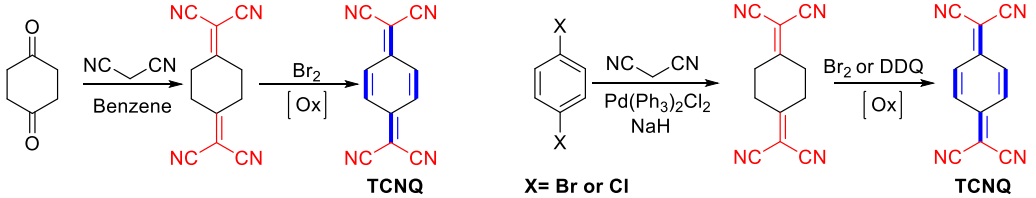

Figure 4. Synthetic route to TCNQ: left the original TCNQ synthesis and right the Takahashi's synthesis.

By using this reaction, a range of quinoidal compounds have been synthesized, so we restrict the discussion to the most recent advances in TCNQ derivatives during the last four years, (Figures 5-8). Tao *et al*. presented the optimized route for the synthesis of quinoidal diketopyrrolopyrrole (DPP) derivative (DCM-DPP-C_{13})[27]. They found that the use of a large amount of sodium hydride damaged the DPP-C_{13}-Br core, which is in sharp contrast with a previous study that used four equivalents of NaH[28]. Additionally, the reaction of the malononitrile anion with DPP-C_{13}-Br over 0.5 equivalent amount of Pd catalyst, distinguished from the typical Takahashi conditions which merely require 1% of catalyst. The intermediate product can be further transformed into the resulting quinoid structure using the strong oxidant, i.e. saturated aqueous Br_2 solution, accompanied by a small amount of bromination of the by-product at the C4 position of the thiophene ring.

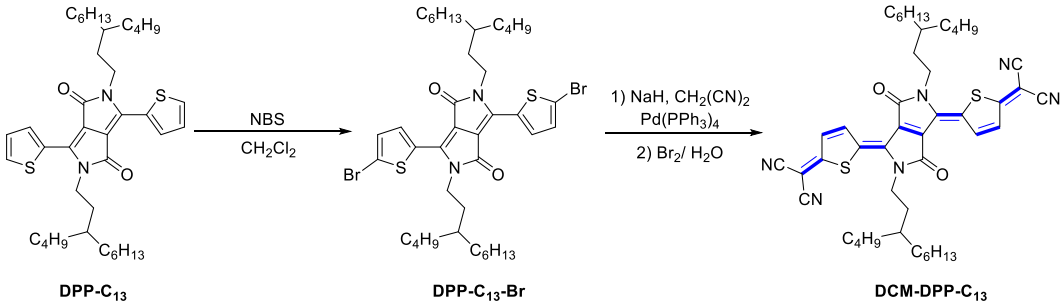

Figure 5. The synthetic route to dicyanomethylene end-capped DPP derivatives.

Jiang and co-workers designed and synthetized S, N-heteroacenes quinoidal compounds (JH06–10, Figure 6)[29]. They have examined the structure-property relationship by investigating the effect of the central heterocyclic core's length on the optoelectronic properties. By altering the quinone core structure the key advantages are shown: Firstly, the N-alkyl substituent of pyrrole provides more solubility-enhancing groups; secondly, the number of species in this family of materials is greatly enriched; and finally, the alternating pyrrole and thiophene units and the electron-withdrawing terminal groups ensure a suitably low LUMO energy level of -4.22 eV.

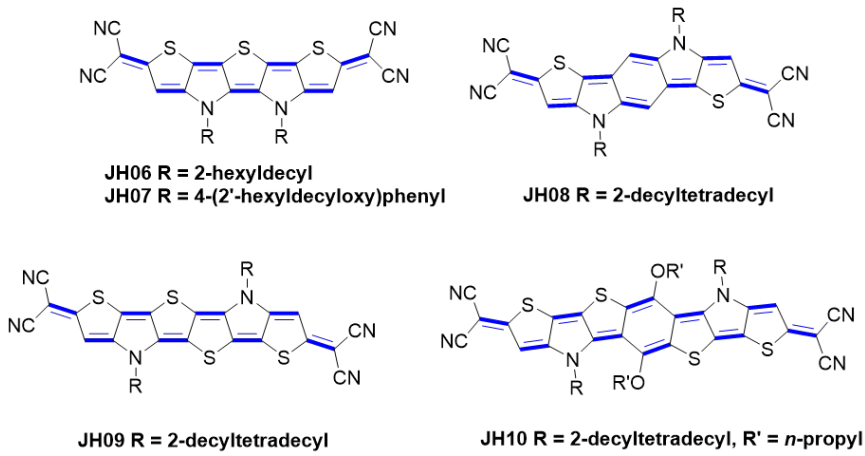

Figure 6. Molecular structures of dicyanomethylene end-capped quinoidal S, N-heteroacenes derivatives.

Joseph and co-workers reported the synthesis of one type of thioalkyl-substituted bi- and ter-thiophene compounds (TSBTQ, DSTQ) with varying chain lengths for OFET applications (Figure 7)[30, 31]. These molecules display a planar molecular structure with short intermolecular stacking distances. In addition, they possess a deep LUMO (<-4.0 eV) that inhibits air oxidation, resulting in excellent ambient stability. The deeper LUMO of -4.28 eV exhibited by DSTQ is due to a downward shift of 0.1 eV in the LUMO energy level caused by the introduction of the sulphur atom into the alkyl side of the molecule, compared to -4.18 eV for the alkylated analogue, with the HOMO energy levels of both also being somewhat affected. The replacement of the terthiophene spacer with bithiophene shows the same trend, and compound TSBTQ exhibits a low LUMO energy (−4.36 eV). These are in accordance with the previously work of Caneci *et al*. who concluded that the insertion of electron-donating group (EDG) onto π-conjugated bridge stabilized the quinoidal (closed-shell singlet) ground state to a great extent and increased the FMO energy levels[32].

The thioalkylthiophene is arranged in a face-to-face slipped π-π stacking arrangement, and the stacking distance of only 3.55 Å facilitates efficient charge transport. The shortest intermolecular distances for S···N and S···S of DSTQ-3 are 3.56 and 3.93Å respectively.

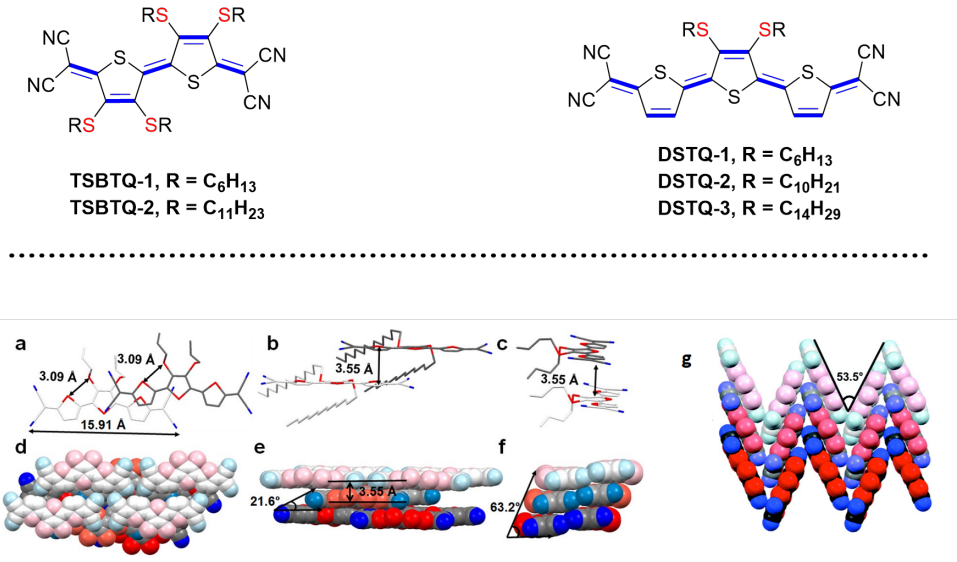

Figure 7. Top: Molecular structures of bithiophene and terthiophene-based small molecule quinoids TSBTQ and DSTQ; Bottom: Representative molecular packing modes of thiolakylated quinoidal oligothiophene: terthiophene and bithiophene (a-c) Top view, front view and side view of DSTQ-3; (d–f) Molecular packing arrangement of DSTQ 1-3; (g) A herringbone mode of TSBTQ-1. Reproduced with permission [30].

Longer π–quinoidal molecules possess singlet open-shell diradical character with one of the outstanding behavior being the formation of the reversible diradical σ-dimer. Recently, Badia-Dominguez *et al*.[33] synthesized and characterized of ICz-CN with dicyanomethylene as the terminal unit at the 3,9 position, which is capable of forming σ-dimer configuration with two coplanar units with intriguing π-π interactions (Figure 8). They highlighted the properties of the open shell forms with respect to their σ-dimers (from ICz-CN to (ICz-CN)2). The reversibility of the monomer/σ-dimer transition was explored in the solid and solution states by varying the external stimulus (temperature or

pressure), respectively. The chemistry of stable σ- and π-dimer of OSC radicals will be discussed in more detail in section 3.7.

To stabilize the quinoidal electronic structure to counter the diradical structure, Yamamoto and coworkers designed and prepared BTQ-3 and BTQ-6, which have a benzo[c]thiophene core [34,35]. In order to avoid the problem of instability of the repeated thiophene framework, the reverse Diels-Alder reaction (220 °C and under reduced pressure) was used in the final step of the synthesis. The diiodide derivative intermediate was oxidised using DDQ following a Takahashi's Pd-catalyzed coupling reaction. The electron accepting ability of these molecules was further strengthened by the insertion of a fluorine substituent at the β-position to the quinoidal skeleton.

Thieno-isoindigo units have been employed extensively as receptor blocks for the OSC materials. The thiophene-based structure is more planar due to reduced intramolecular space resistance compared to the benzene ring, while the thiophene-thiophene linkage along the backbone maximises the conjugation length and further enhances the intermolecular tight contacts. A series of dicyanomethylene end-capped quinoidal thieno-isoindigo with various alkyl chains (TIIQ) was synthesized by Facchetti group. [36] It was identified that the strategy of varying the branching points of the alkyl side chains resulted in varying the intermolecular stacking distances, which slightly tuned the optical and electrochemical properties of the resulting materials. These molecules are typically characterized by a very low LUMO energy level and show a mobility of up to 2.54 $cm^2 V^{-1} s^{-1}$ in OFET devices.

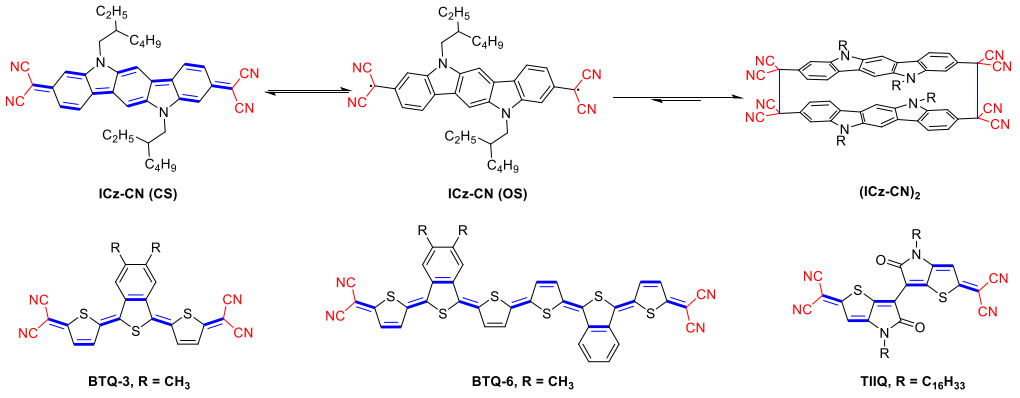

Figure 8. Molecular structures of ICz-CN (top), BTQ-3, BTQ-6, and TIIQ.

3.2. Indandione terminated π-conjugated small molecules

An alternative kind of quinolone moiety consists of indandione units capped are shown in Figure 9.[37, 38]. These compounds feature low lie LUMO levels below -4.0 eV and their LUMO levels are less affected by the central core π-bridge, the reduction in the band-gap of the material is mainly attributed to the rising HOMO levels as the π-conjugation increases. All these materials showed unipolar electron transport behaviors, exhibiting a maximum μ_e of 0.38 $cm^2V^{-1}s^{-1}$.[39]

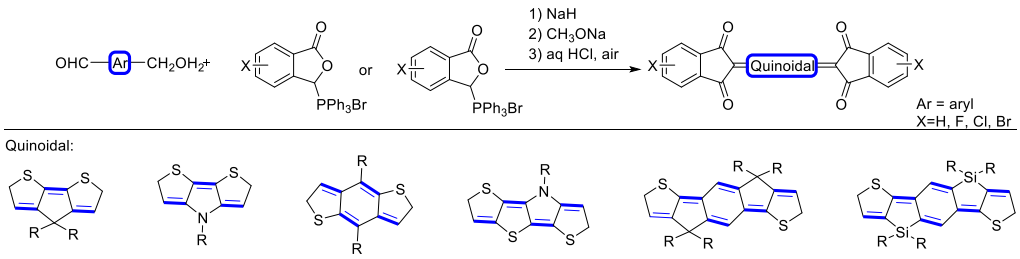

Figure 9. The synthetic route to construct indandione-terminated quinoidal materials.

3.3 Analogs of Thiele's and Chichibabin's dyes

Among various classes of quinoidal OSC, Thiele (p-quinodimethane), and Chichibabin, polycyclic aromatic hydrocarbons have been extensively studied. They can be considered as the first known quinoidal dyes. X-ray analysis of such molecules demonstrates a planar π-di-xylylene structure, which indicates a major contribution from the quinoidal resonance form in the crystal[40]. The length of all the bonds in the fundamental backbone lies in the range 1.371-1.448 Å, between the double and single bond values. In addition to this, the four benzene rings are rotated by an average of 43° rather than being aligned coplanarly. Given these structural findings, the improved kinetic stability of the Thiele hydrocarbons with respect to the parent may be largely due to steric effects. This feature is of considerable importance in the evaluation of design standards, synthesis and purification of new analogues of Thiele and Chichibabin hydrocarbons. In synthesizing such quinoidal hydrocarbons several modifications of initial procedures were attempted. Some were successful; some were not. Initial studies involving 4,4'-Bis(diphenyl-hydroxymethyl)biphenyl required the use of n-butyllithium and the resulting diol intermediate was subject to zinc debromination, but in very low yields. An alternative procedure employs the bis-carbenium salts, obtained by the protonation of the corresponding diols, which were successfully converted to the corresponding quinoidal compounds in good to reasonable yields (Figure 10)[41,42]. The stability of di-carbocations is an issue in the above synthetic approach. To overcome this shortcoming, Takeda T. *et al*. improved the product's overall yield[43]. Thus, for the dehydration step, they changed the Brønsted acidic, $HClO_4$ to a soft Lewis acid $TMSClO_4$, to generate the corresponding dicationic species. The corresponding target products were successfully obtained by treating the diols with $TMSClO_4$ and then reducing with Zn. The yield of the dehydration step was raised sharply from 6% with $HClO_4$ up to 99% with $TMSClO_4$. The impact of terminal segments has been discussed, involving dibenzocycloheptatriene, fluoryl, and cyclopentadithiophene. Kobayashi *et al*. reported a variety of synthetic methods to prepare quinoidal systems fluorenyl end-capped. Three different approaches have been used for the generation of quinoidal derivatives, chemical, photochemical and thermal.[44]

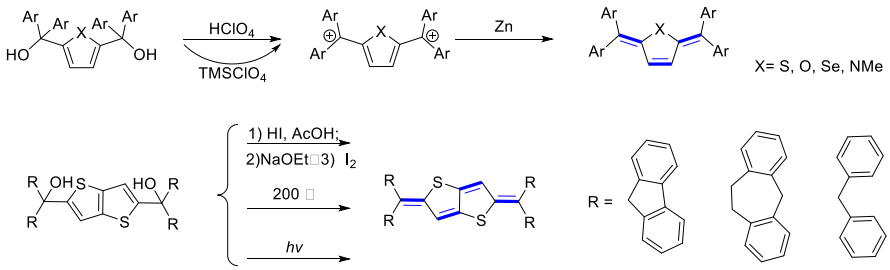

Figure 10. The synthetic route to Thiele's and Chichibabin's hydrocarbons.

Recently, an example of cyclopentadithiophene (CPDT) unit incorporated as an end group on the quinoidal structures allowing fine-tuning the FMO energy levels of the molecular components was reported by Wang and coworkers[45]. Even though CPDT is more donating than fluorenyl, the introduction of this group as a terminal part of quinoidal frameworks has noticeable stabilizing effects on the HOMO level, while the LUMO remains almost unaltered. The chemistry used to introduce this building block is similar to that of fluorenyl, based on the diols intermediates (Figure 11). The diols were synthesized by the double lithium-halogen exchange in di-halogenated aromatic and subsequent nucleophilic addition to aromatic ketone affording diols. The quinoidal structures were then attained in moderate yields through the reduction of the diol by $SnCl_2$ in THF. We note that the diol intermediates were further reduced, neither isolation nor purification, which greatly simplified the synthesis process. A similar protocol was used in the synthesis of Thiele and tetrabenzo-Chichibabin derivatives with terminal dibenzocycloheptatriene units (DBHept) [46].

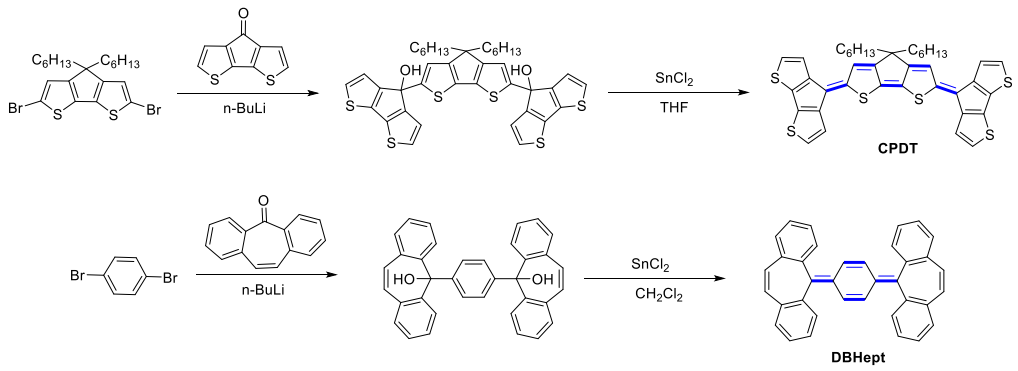

Figure 11. The synthetic route to CPDT and DBHept quinoids.

3.4. Synthesis of indophenine dyes and oxindole end-capped quinoidal molecules

Adolph von Baeyer illustrated in 1879 that combining red isatin with benzole under sulfuric acid conditions generates the result of a deep blue compound, named indophenine [47]. Victor Meyer subsequently investigated thiophene in his study of this reaction and identified indophenine as the composition of isatin and thiophene. [48]. The thiophene comes from the small amount of contaminants present in the benzole and the blue product is not composed of isatin with benzene as was initially thought. One century later, in 1993 Tormos *et al*.[49] suggested the presence of six stereoisomers of N-alkylated indophenine in solution by analysis of two-dimensional COSY Spectroscopy, as shown in Figure 12. Since these works, little interest has been dedicated to research in this area because the pre-existence of isomers affects the behaviors of molecular self-assembly and highly crystalline films are in direct correlation with the mobility of the charge carriers.

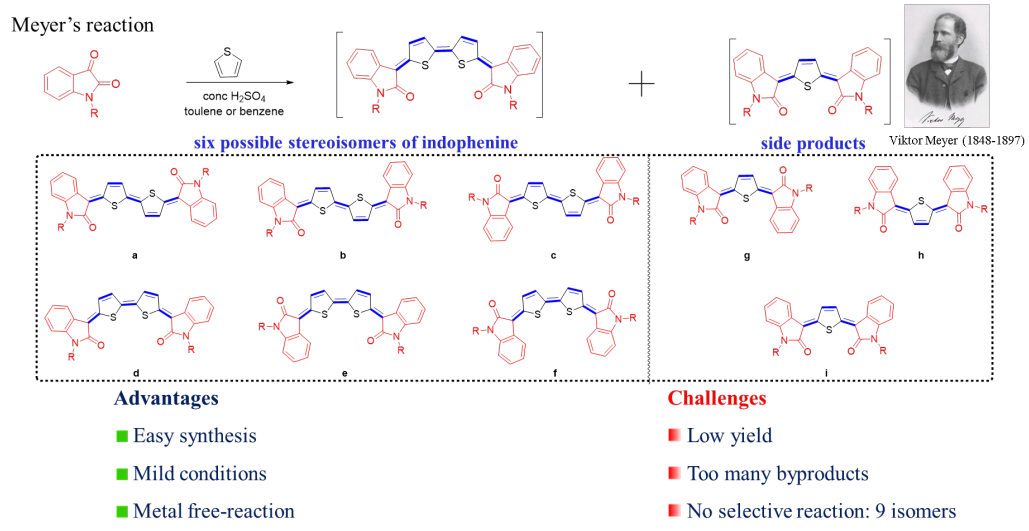

Figure 12. The classical method to the preparation of indophenine dyes.

The straightforward synthesis of indophenine molecules is acid-catalyzed condensation of isatin with thiophene (synthesis route A, Figure 13). Hwang and coworkers synthesized compounds 1a-1f and 2a-2f, whereby the quinoidal thiophene and selenophene were served as bridging groups respectively.[50]. They demonstrated that the different isomers own different characteristics in HOMO and LUMO energy levels. The trans-isomeric configuration between the thiophenes is energetically lower and therefore more stable compared to the cis-isomer. Although the simplicity of the synthetic approach to indophenine, the formation of isomers leads to challenging purification of the final product

and low yields of the reaction. In practice the reaction results in two types of quinoidal molecules with dissimilar core lengths tending to be produced simultaneously, further decreasing the yield of the desired target product (compounds 1a-1f, 6 isomers and compounds 1g-1i, 3 isomers), in yield of ~36% and ~18%, respectively [51,49]. The quinoidal thiophene, regarded as the side-product, was separated and characterized by 2D NOESY NMR spectroscopy, which revealed that the main isomer showed an asymmetric *Z*, *E*-configuration[51]. Most recent investigations have shown that the dipole repulsion between the carbonyl groups in compound 6g (*Z*, *E*) is the smallest of the three. Likewise, among the theoretical six geometric isomers, the quinone bithiophene with the (*Z*, *E*, *Z*) form is considered to be the major product[52]. Their dyeing behaviors, optical properties and light stability were studied by Chen *et al*. who investigated the influence on halogen substitution (-F, -Cl), as well as the -SO_3H (compounds 3-5) in oxindole moiety on the photophysical properties and dyeing performance [53, 54]. The location where the quinoidal skeleton occurs was studied by Bhanvadia *et al*.[55] They found that under similar experimental conditions, the product formed using a catalytic amount of concentrated H_2SO_4 was actually 6k rather than 6j. The quinoidal structure existing on the pyrroloindole dione unit was related to the steric bulk caused by the bromine substituents. One alternative approach for the synthesis of indophenine has been advanced by Ren *et al*. (route B) [56,57]. This reaction involves Sn^{II}-mediated reductive aromatization of diols to afford the fully conjugated quinoidal products with subsequent oxidation of the intermediate aromatic intermediate. For instance, the aromatic ring containing the lithium substituent is added nucleophilically to the carbonyl group of isatin to obtain the diols intermediate, in a good yield, followed by reductive aromatization using $SnCl_2$ reduction. Dehydrogenation using DDQ produced compound 7a-7c as a mixture of three isomers. It should be noted that the reduction of the diols by $SnCl_2$ can also lead directly to the quinoidal form, 7a-7c, depending on the reaction conditions (route C)[58].

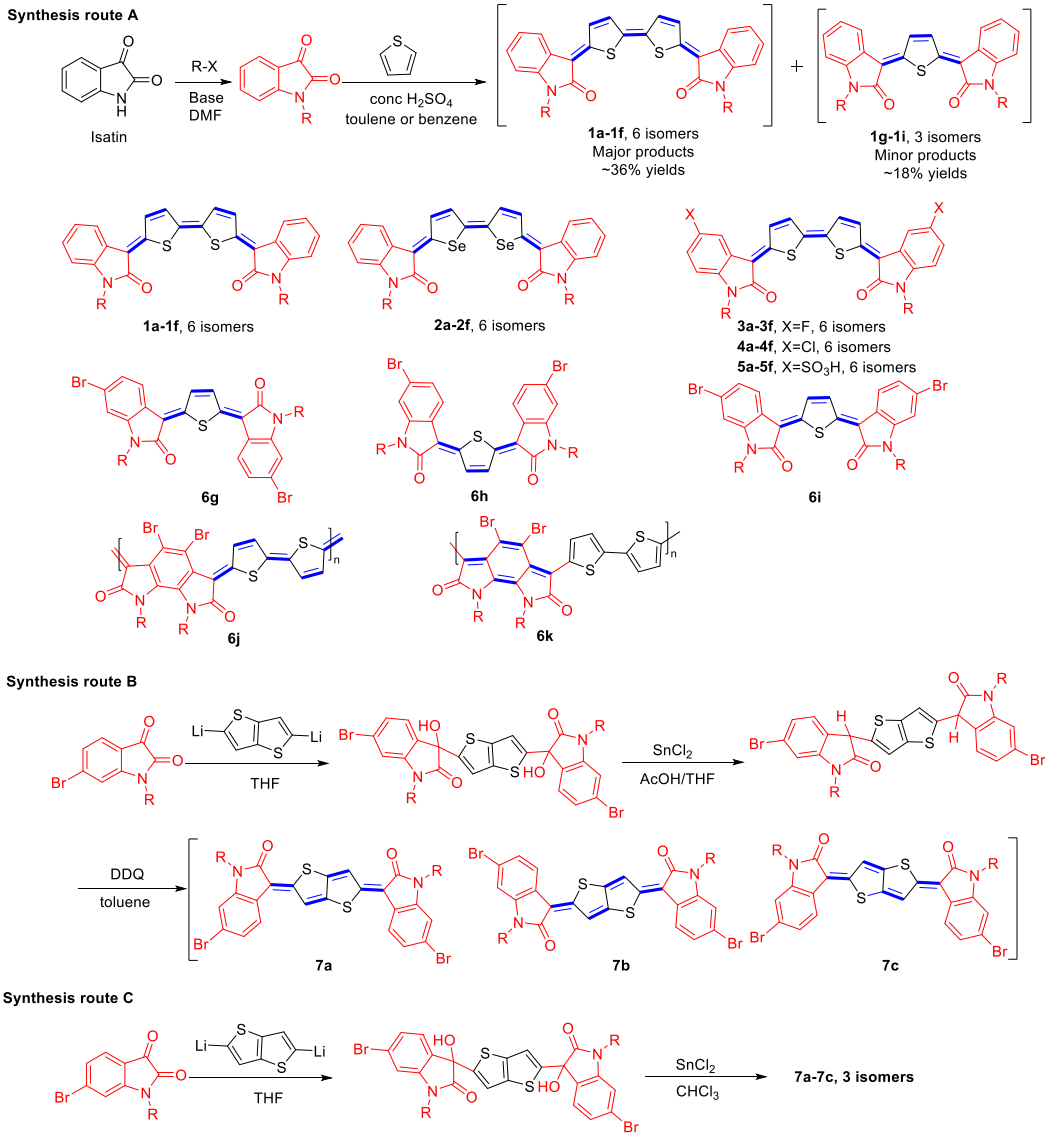

Figure 13. Different synthesis routes for the preparation of indophenine and their chemical structures of indophenine dyes isomers reported in the literature.

Three approaches have been used to overcome the severe issue of stereochemistry. For the first method, it relies on the steric hindrance obtained by the oxidation of thiophene thereby reducing the amounts of isomers. Deng *et al*. found that the oxidation of thiophene unit in indophenine system provided a dual benefit: (i) a significant drop in both LUMO and HOMO; (ii) facilitated isomerisation yielding a single isomeric product.[59] As shown in Figure 14, 3-chloroperoxybenzoic acid (*m*-CPBA, route D) was employed to oxidize a mixture of 8a-8c, followed by refluxed in toluene to afford a pure single isomer of indophenine (compound 9c). This is because 9c is the most stable form among the three isomers. On the other hand, the isomerization process from 9b or 9a to 9c is accelerated under mild heating conditions. Compared to compound 8, the HOMO energy level of oxidization quinoidal compound 9 was significantly lowered to –5.91 eV (Table 1). Finally, the pure isomer was used as a co-monomer feed for constructing polymer (P1, Figure 15). P1 exhibits the narrow band-gap together with the low energy levels (LUMO: -3.98 eV & HOMO: -5.92 eV). P2 and P3 were synthesized later, and it was noteworthy that P2 has a deeper LUMO of -4.09 eV compared to that of P1.The LUMO level was further reduced to -4.18 eV by introducing 2,2'-bithiazole (BTz) into the D-A polymer system (P3), which serves as the electron donor.[60] A impressive study of the impact of S, S-dioxided thiophene on the opto-physical and electrochemical properties of indophenine derivatives was

reported by Hu and coworkers[61]. They synthesized several thiophene-S, S-dioxidized indophenine substituted at 5,5' positions with electron donating/withdrawing groups (compound 10a-10e). It was concluded that: (i) oxidation of thiophene significantly improved the structural stability; (ii) insertion of S, S-dioxidized unit in quinoidal system caused a significant hypsochromic shift in the absorption; (iii) EDGs were beneficial in maintaining the quinoidal state, whereas EDGs had strong influence on the electron cloud density distribution. It was well known that the 5,5' position was a cross-conjugated isoindigo, and therefore the π-electrons were not well delocalized over the entire molecule, which dramatically affected the properties of the molecule. The impact on cross-conjugation of the substitution pattern on the electronic properties was investigated by Deng[62]. Compared to unsubstituted 11a, the substitution at 5- or 6- position lowers the FMO energy levels, however, the position of substitution has little effect. The DFT calculations revealed that the substitution at 6,6'position (compound 11b) participates in LUMO and HOMO conjugation paths by inductive/ resonance effects. While, 5,5'-dibromo substituents, compound 10c, only participate in the HOMO wave function through the inductive and resonance effects. The charge transport properties are found to be less impacted by the position of the substitution. The electron mobility of the molecule substituted at position 5 rising up to 0.071 $cm^2 V^{-1} s^{-1}$ a value comparable to that of compound 11b, 0.11 $cm^2 V^{-1} s^{-1}$, although the compound 11b has a more extended π-conjugated system. Geng's group further expanded the range of products obtained by relying on this type of synthetic strategy (route D). Oxidation of the mixture 7a-7c with *m*-CPBA, followed by thermal isomerization (120℃ in toluene), gives a single-isomer (compound 12c).[56] Bromine functionalized isatin derivatives can be further used to design more sophisticated macromolecular architectures, and three different donors were introduced into the synthesis of three polymers, P4-P6 (Figure 15). The LUMO level of these polymers is constant at -4.04 eV. While on the one hand, they show a variation in HOMO from -6.00 to -5.91 eV because of the different donor abilities of donor-acceptor (Table 2). Upon substitution of peripheral hydrogen atoms with fluorine in the terminal isatin units, the resulting fluorinated indophenine dyes exhibited lower LUMO/HOMO levels.[63]. Compound 13a-13c with varying amounts of fluorine substituents on the oxindole have been reported. All derivatives exhibit n-type transport behavior, where the electron mobility is correlated with the number of fluorine atoms. 13b exhibited the highest electron mobility of 0.16 $cm^2 V^{-1} s^{-1}$ which is associated with its two-dimensional electron transport mode and highly ordered film.

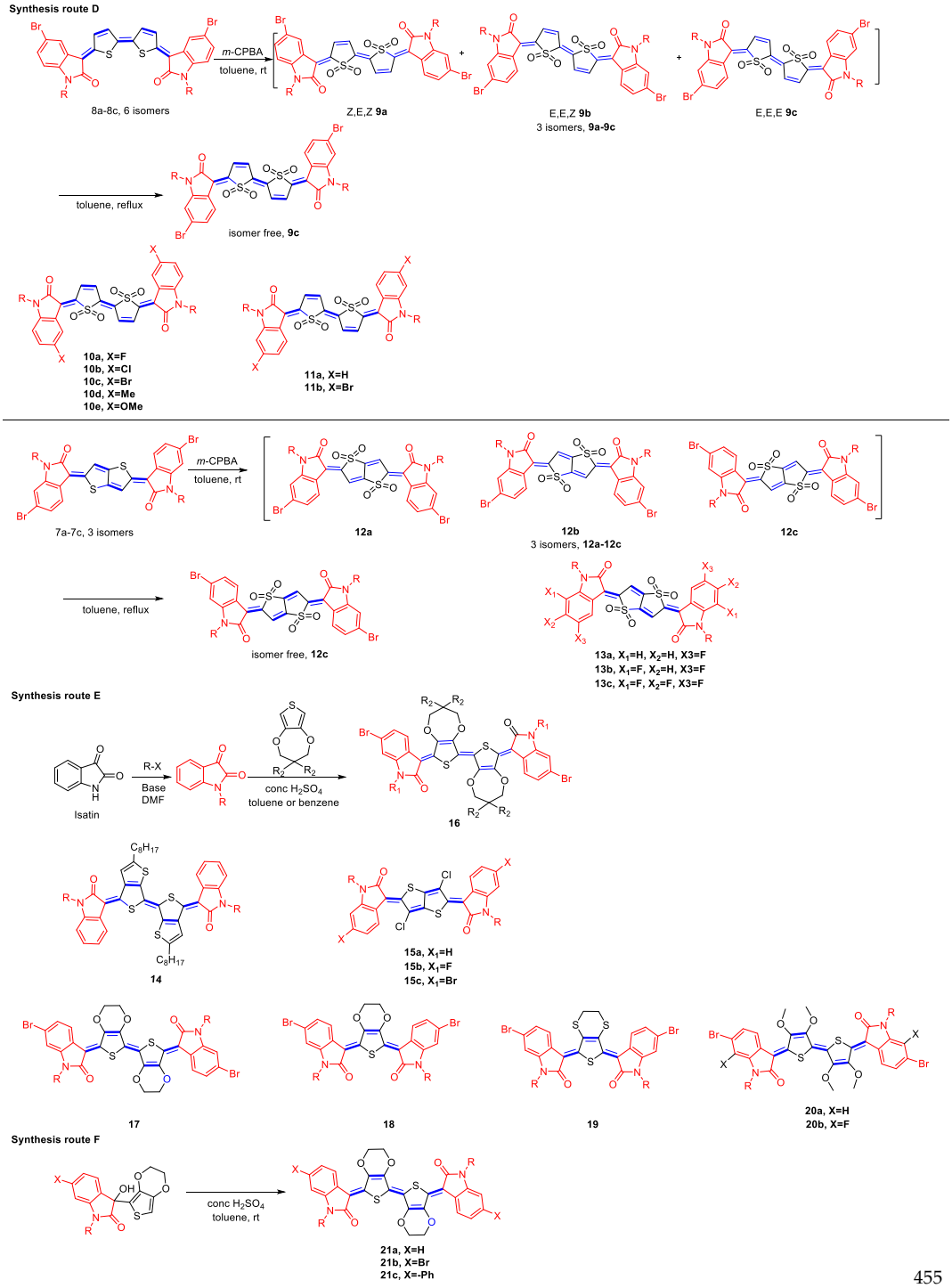

Figure 14. Different synthesis routes for the preparation of isomerically pure indophenine dyes and their chemical structures reported in the literature.

The second method employed to drive the reaction to single isomer formation involves the utilization of non-covalent conformational locking and steric repulsion as the driving forces. The original synthesis of indophenine involved the condensation of thiophene and isatin under concentrated sulfuric acid. Nevertheless, this condition resulted in a complex mixture as reported by Cava *et al*[49]. This limitation was elegantly overcome by Ren and coworkers, who proposed mild reaction conditions using Sn^{II}-mediated reductive aromatization of diol to afford the fully quinoidal form (compound 14) without oxidation of the intermediate aromatic form[57]. For the final step, air oxidation led to the formation of targeted compounds in good yield, although the authors did not mention the

role of oxygen in their discussion. The intramolecular O···H interactions present in the compound 14 and confirm a well-defined conformation, as shown in the Figure 14, with no other isomers generated. The thieno[3,4-b] thiophene favours the stable *E* conformation, its large π surface and short intermolecular S···S interactions also favour hole transport. p-type semiconductors compound 14 exhibited excellent unipolar hole mobility up to 0.15 $cm^2 V^{-1} s^{-1}$. Geng's group further proposed the chlorination strategy for the conformation of the locked indophenine derivatives[64]. The energy gap among 7a-7c was determined by DFT calculations to be less than 1 kcal/mol, and this variation was significantly enhanced by the insertion of a chlorine atom. By using non-bonded covalent interaction analysis, it was shown that although, there are certain S···H and O···Cl interactions, the Cl···H and S···O interactions tend to be stronger. The maximum absorption peaks of 15b and 15c were red-shifted compared to 15a, and the introduction of F and Br reduced E_{HOMO}/E_{LUMO} significantly (Table 1).

Table 1. Molecular optical properties and electrochemical characteristics of small molecular based on indophenine reaction derivatives.

Materials	λ_{max}^{sol} (nm)	λ_{max}^{film} (nm)	$E_g^{opt\text{-}film}$ (eV)	E_{HOMO} (eV)	E_{LUMO} (eV)	E_g (eV)
8	600	650	1.55	-5.41	-3.86	1.55
9	450	500	1.83	-5.91	-4.08	1.83
10c	479	497	1.67	-6.33	-4.12	2.21
11a	476	491	1.74	-5.85	-3.99	1.86
11b	482	507	1.72	-6.30	-4.18	2.12
13a	427	423	1.81	-5.98	-4.17	1.81
13b	431	427	1.85	-6.10	-4.25	1.85
13c	430	425	1.82	-6.14	-4.32	1.82
14	665	618	1.56	-5.10	-3.58	1.52
15a	542	467	1.65	-5.47	-3.97	1.54
15b	606	475	1.63	-5.53	-4.01	1.56
15c	620	486	1.56	-5.58	-4.05	1.53
16	650	-	1.44	-5.30	-3.86	1.44
18	537	-	1.95	-5.29	-3.47	1.82
19	592	-	1.79	-5.33	-3.73	1.60
21a	633	-	1.67	-5.10	-5.39	1.71
21c	661	-	1.55	-4.85	-3.40	1.45

Further development of the selective synthesis of a single isomer was accomplished by Pappenfus *et al*., who succeeded in producing a single isomer using the noncovalent conformational lock approach. Route E outlines the reaction of N-alkylisatin with 3,4-propylenedioxythiophenes (ProDOT) in toluene catalyzed by sulfuric acid to form quinoidal molecular (compound 16). The intrarmolecular interaction was the driving force for obtaining one of the isomers [65]. Using a similar strategy, O···S non-covalent interactions and steric repulsion were employed towards the synthesis of bis-QEDOT, compound 17[66]. Similarly, Kim *et al.* found that 17 and 18 were synthesized simultaneously by the indophenine reaction under sulfuric acid catalytic conditions with yields of 40% and 12%, respectively.[67] Both quinoid monomers were confirmed to have a single geometric structure by NMR analysis, which also confirms the intramolecular nonbonding S···O interactions. P7 and P8 have been obtained by polymerization reaction using mono- and di-EDOT with vinyl. The substitution of O atoms in the quinoidal core by S atoms in compound 19 improve π-electron accepting ability of the system.[68] The S-based analogs exhibit lower FMO levels with narrowed band-gaps. However, the authors noted that 19 has two isomers, meaning that it can be isomerized under ambient conditions due to the low activation energy of quinoidal molecules. The corresponding monomers were polymerized with bithiophene to obtain polymers P9 and P10, respectively. The Grazing incidence wide-angle

X-ray scattering results showed P9 film with ordered crystallization and better hole mobility in the OFET. Most recently, the substitution of the H with methoxy group on thiophene was promoted in the O···S conformational locking of indophenine[69]. In addition, three polymers consisting of bis-QEDOT (P11-P13, Figure 15) were synthesized by a Stille polymerization reaction. The high HOMO energy level of these polymers, close to -4.5 eV, makes them promising p-type OFET materials. After substitution of methoxy at the 3,4 position of thiophene, the reaction gave only a single *Z*, *E*, *Z* conformation of product 20. The X-ray structure shows a highly planar core with a distance of 2.69 Å between the S and O atoms, indicating the involvement of spatially non-covalent interactions, which leads to a dihedral angle of almost 0° between the two thiophene molecular units.

Recently we have developed the idea of a novel variant of the indophenine condition [70]. The previously reported route involved a one-pot procedural process starting with isatin and a suitable 5-membered aromatic heterocycle. However, as we have discussed above, the yield under this condition was low and the selectivity poor. We propose to modify the standard conditions to improve the yields by using tertiary alcohols as starting materials (Compound 21a-c in Route F). This strategy proved to be particularly selective, isomer-free for the synthesis, avoiding any complex purification problems, all of which resulted in the product yield being improved. A range of quinoidal materials with variable termini and modified conjugate cores have been synthesised and characterised.

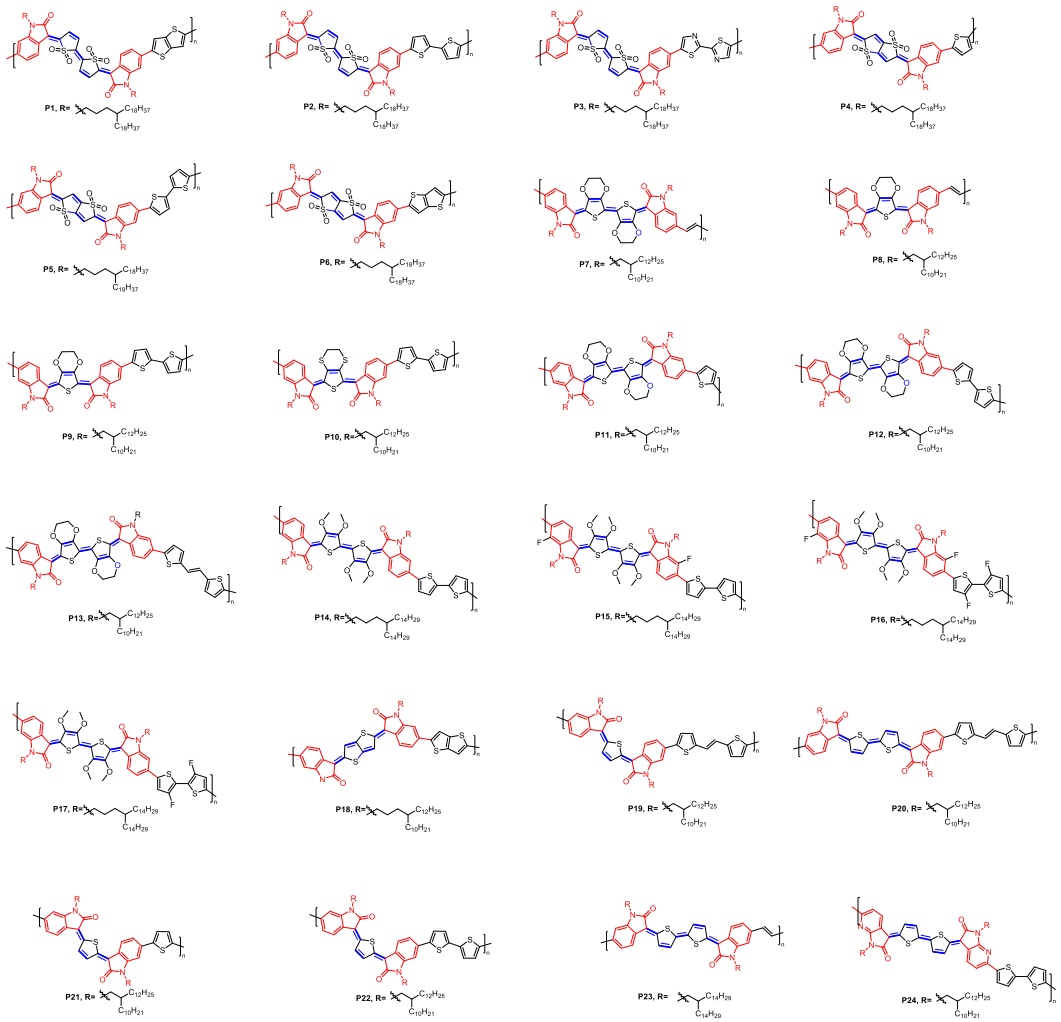

Figure 15. Chemical structures of copolymers based on indophenine dyes reported in the literature.

Table 2. Optical properties and energy levels of conjugated copolymers based on indophenine dyes.

Materials	λ_{max}^{sol} (nm)	λ_{max}^{film} (nm)	$E_g^{opt\text{-}film}$ (eV)	E_{HOMO} (eV)	E_{LUMO} (eV)	E_g (eV)
P1	710	710	1.42	-5.92	-3.98	1.94
P2	780	-	1.43	-5.78	-4.09	1.69
P3	636	-	1.62	-5.99	-4.18	1.81
P4	740	723	1.48	-6.00	-4.04	1.96
P5	751	740	1.47	-5.95	-4.03	1.92
P6	758	750	1.43	-5.91	-4.05	1.86
P7	811	821	1.17	-4.59	-3.62	0.96
P8	753	748	1.52	-5.14	-3.62	1.52
P9	670	743	1.52	-5.17	-3.58	1.59
P10	723	787	1.36	-5.17	-3.70	1.47
P11	787	794	1.15	-4.58	-3.43	1.15
P12	746	752	1.16	-4.52	-3.36	1.16
P13	728	712	1.18	-4.50	-3.32	1.18
P14	760	758	1.18	-5.31	-3.95	1.36
P15	984	965	1.15	-5.35	-3.92	1.43
P16	936	930	1.13	-5.43	-3.97	1.46
P17	892	794	1.14	-5.32	-3.92	1.40
P18	876	910	1.28	-5.19	-3.63	1.56
P19	728	778	1.34	-5.22	-3.43	1.79
P20	774	900	1.16	-5.04	-3.65	1.39
P21	768	773	1.44	-5.24	-3.56	1.68
P22	773	769	1.45	-5.11	-3.55	1.56
P23	807	829	1.12	-5.08	-3.79	1.29
P24	845	981	1.11	-5.03	-3.74	1.29

3.5. Molecular and electronic structures of oxindole terminated quinoidal molecules: electrochemical and optical properties

Indophenine dye is an electron-deficient building block which can be regarded as an isoindigo analogue with a central π-core extension. It contains two electron-withdrawing carbonyl units of oxindole moiety to gain better stability for the π-extended quinoidal structures also provide a deep LUMO level (–4.0 eV) [71]. The indophenine structure after DFT optimization indicates an nearly planar skeletal configuration [53]. The electron cloud density is mostly delocalized over the quinoidal π-system. The FMO levels are sensitive to the variation of the substituents. The general trend is that an EDG can increase the energy level while the EWG plays the opposite role. For instance, by introducing a halogen atom (fluorine or chlorine) on benzene of oxindole ring, the energy level of the material is correspondingly and significantly reduced. Another promising method for tuning the electronic energy levels of indophenine molecules is to alter the quinoidal π-conjugated core. To illustrate this, Hu and coworkers assessed the energy levels in a series of substituted indophenine compounds where the sulfur atom of thiophene is oxidized to the S, S-dioxided thiophene. From DFT calculation and electrochemical study, a shift of 0.5 eV of the LUMO levels is observed, which clearly demonstrated the strong electron affinity of compound 12c. Replacing of the thiophene in indophenine molecule with ProDOT or EDOT resulted in materials with similar LUMO levels, Table 1. The variation in HOMO in compound 16/17 can be explained by the strength of the electron donating capacity of ProDOT/EDOT vs. thiophene group.

3.6. Crystal packing of indophenine molecules with O···S conformational locks

In OSCs, the non-covalent conformational lock has been employed as a practical means of improving the planarity of the skeleton, enhancing molecular stacking and

improving the mobility of charge carriers. Components bearing O···S non-covalent interactions are already extensively employed as conformational locks to construct OSCs, and there are many examples of EDOT-based materials with an O···S bond locked conformation. For instance, bi-EDOT's crystal structure indicates intense intramolecular non-covalent interactions[72]. Analysis of its crystal structure allows calculation of a distancing of 2.92 Å between the O and S inside the molecule, which is smaller compared to the sum of the van der Waals radii of the two atoms. This force locks the conjugated structure into an almost planar conformation with a torsion angle of 6.9° (Figure 16a). Another system where intramolecular O···S forces are also present is based on the dicarboxylic-bithiophene moiety. Figure 16b illustrates the intense forces that exist within the molecule due to the close spatial distance of the S···O, resulting in a near-flat skeletal structure with a minor torsion angle of 2.7°. Likewise, the double ProDOT core in compound 16 favors a macroplanar structure throughout the entire molecule, with an infinitely sliding layer-by-molecule arrangement of an interplanar distance of just 3.57 Å (Figure 16c). Figure 16d illustrates that the distances between the S atom and the two adjacent O atoms within the molecule are 2.670 and 2.788 Å, respectively, and that those contacts are obviously shorter than the sum of the van der Waals radii of S and O (3.25 Å).

What is interesting is that the controlled generation of isomerisation to the single isomer 9c is promoted in compounds 9a-9c due to the introduction of steric hindrance[73]. Figure 16e analysis further confirms that the isomers adopt the *E*, *E*, *E* conformation and exhibit a completely planar skeleton. The introduction of two additional O atoms in each thiophene presents an almost perpendicular angle to the entire plane. These molecules form of a sliding face-to-face stacking pattern with an interlayer distance of 3.76 Å. Intermolecular hydrogen bonds have been formed between the H_4 proton of the thiophene and the O atom of the oxindole unit, measuring the H to O distance and the angle of this bond at 2.457 Å and 128.58° respectively (Figure 16f). By replacing the π-bridge of indophenine dye, bis-EDOT unit (compound 17), with tetra-methoxy-bithiophene (compound 20a) a single regio-isomer was obtained, [74] via the manipulation of the configuration by a joint effect of steric hindrance and intermolecular contact to lock the conformation. Thus, according toFigure 16g, compound 20a molecule exhibits an almost planar structure and maintains the *Z*, *E*, *Z* conformation, with a torsion angle of only 6.7° between isatin and DMOT. The spatial distances between the two O atoms and the central S atom are found to be 2.84 and 2.69 Å respectively. As previously discussed, the contact of S···O highlighting again the role of intramolecular non-covalent interactions in the conformational lock. The role of intramolecular interactions to induce conformational lock was further demonstrated in di-chlorinated bithiophene bridge in indophenine (compounds 15a-c)[64]. The presence of intramolecular Cl···H and S···O non-covalent interactions in Figure 16h contributes to the stabilisation of the *Z*, *Z* conformation.

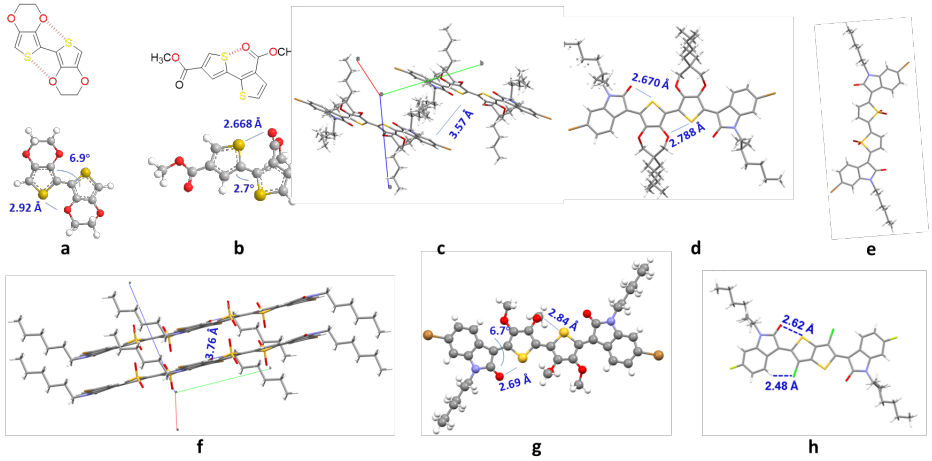

Figure 16. Representative examples of indophenine dyes with different conjugated π-bridge cores showing conformational locking. Adapted with permission from references [72,65,74,64].

3.7. Chemical stability of diradicals based quinoidal molecules

Although quinoidal molecules have emerged as excellent ambipolar and n-channel OFET materials, only little literature exists on their stability. In fact, In fact, such materials are commonly thought to present two types of resonance structures, one quinoidal and the other diradical. Diradical structures contain at least one unpaired electron, which renders them more reactive and sensitive species, they are so facing stability issues[75]. Few studies from different groups: Haley [76], Wu [77], Chi [78,79], Casado [80], Tobe[81] and Navarette [82] have shed some light on the stability of diradical hydrocarbons, providing guidelines on how to design stable diradical π-conjugated materials. The major challenge in designing these materials is to achieve a balance between their stability and targeted properties. Different strategies to stabilize π–radicals are used[83]. Firstly, the kinetic stabilization which consists in introducing a bulky substituent in the close vicinity of the radical center to hinder its dimerization. Spin delocalization approach, π-radicals with more spin delocalization are more stable, because the spin density is diluted which causes diminished reactivities. Finally, the introduction of EDGs which provides thermodynamic stabilization through their conjugative and inductive effects. Dimerization is considered as the main way by which radicals are degraded. This can be categorized as: σ- and π-dimerization. The former involves the formation of a covalent (σ) bond between two radicals. The latter, often observed in the association of π-conjugated radicals, and consists of the formation of a stacked pair of radicals via π-orbitals. Some dicyanomethylene end-capped oligothiophenes, at low unit numbers there is a closed-shell quinonidal structure, while as the length of the oligomer increases its ground state is transformed into an aromatic open-shell diradical. These Open Shell structures can reversibly dimerise when stimulated by external concentration, temperature or pressure conditions. In a recent study, Zafra and coworkers demonstrated that quinoidal are capable of forming σ- or π-dimers according to the properties of the terminal moieties. They found that the different conformations of the dimer, such as open, extended and completely closed, were caused by different mechanisms[84] (Figure 17).

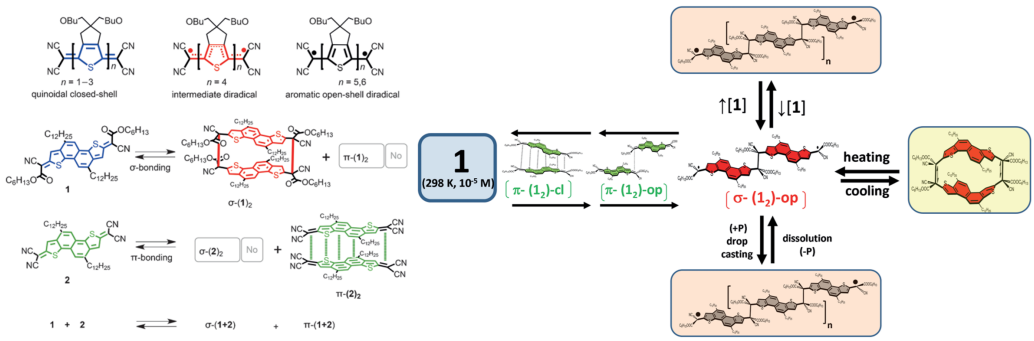

Figure 17. Left: Multiple di-radical properties and combinations of forms of oligothiophenes; Right: multiple conformations and modes of dimerisation reactions Reproduced with permission from ref [84].

A fundamental understanding of how a π-conjugated core impact the reactivity of σ-bonds was reported by Badía-Domínguez *et al*[33]. Diradical ICz-CN forms two long-range σ-bonds between the dicyanomethylene substituent during complete dimerization to (ICz-CN)2., Figure 8. The reversibility of this transformation has been discussed in solid and solution state. Butyl-substituted phenalenyl-based neutral radical materials assume great importance in terms of potential applications. The understanding of their chemistry, as well as the design rule for synthetizing stable open-shell phenalenyl structures have been reviewed [85]. For instance, fusing an anthracene with bisphenalenyl units generates a relatively stable Kekulé molecule with a very significant singlet diradical character[86].

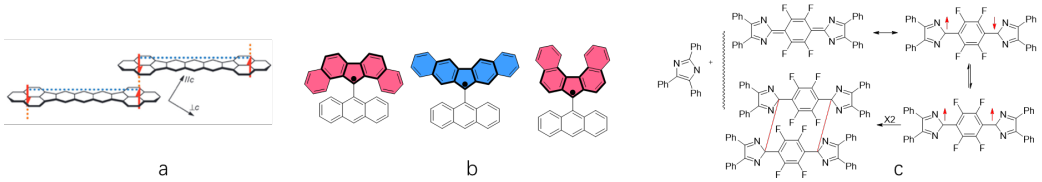

Figure 18. (a) Intramolecular and intermolecular forces present in Kekulé molecules; (b) Three isomers of fluorenyl—naphthalene-1, -2 and -3, based radicals stabilized by stabilized by 9-anthryl group; (c) Photochromic Kekulé hydrocarbon with an imidazolyl radical moiety. Reproduced with permission from ref[86,88,89].

Kubo and his colleagues investigated the correlation between three modes of cyclization and the stability of radicals. They prepared three radicals of fluorenyl fused naphthalene rings, fluorenyl-naphthalene-1, -2, -3, that differ in their mode of annelation [89]. The half-lifetime of the materials for the three models are 7 days, 3.5 days and 43 days respectively. The variation in stability is related to the kinetic stability as well as the thermodynamic stability achieved through the spin-off domain. Bis-imidazolyl radical moiety was recently explored by Abe group as a novel photochromic molecular system[88]. It was revealed a difference in the stability of the singlet and triplet state, and upon excitation at 609 nm, the imidazolyl core dimerizes to the colorless dimer (Figure 18).

In this section we analyzed OSC radicals showing reversible association-dissociation behavior, forming σ- and π-dimer, from the viewpoint of molecular design. The recent studies represent significant advances in understanding the formation of highly stabilized intramolecular dimer radical, σ- or π-dimer by the reversible monomer–dimer transition in the solid state. All these results pave the way to future directions on how diradical character can be controlled or modulated with external stimuli.

4. Device applications

4.1.1. OFET-materials based on dicyanomethylene end-capped quinoidal molecules (n-type and ambipolar)

Since the seminal works of Frisbie *et al*. on the use of dicyanomethylene end capped quinoidal oligothiophenes as active material in n-type OFET, various quinoidal materials have been investigated [90,91]. In the last two decades, an impressive range of OSCs (n-type, small molecules or polymers) have been reported and shown to have high electron mobility (0.5-1.0 $cm^2V^{-1}s^{-1}$). The chemical modification approach has shown to be an effective strategy for synthetizing efficient stable n-type OFETs [92].

Dicyanomethylene end-capped thiophene-based quinoidal compounds are an outstanding family of n-type OSC thanks to the existence of strong EWG at the end of quinoidal structure, affording thus a low-lying LUMO level. The central quinoidal cores promote π-stacking, thus inducing strong non-covalent intermolecular interactions, which may lead to increase the charge carrier mobility. Thus, several groups have explored the use of dicyanomethylene quinoidal molecules as n-type OSCs for OFET application (Figure 19). TIIQ-b16 afford OFETs with good mobility (μ_e = 2.54 cm^2 V^{-1} s^{-1}) [36]. In this molecular structure, the quinoidal structure resulting in a low-lying LUMO energy (−4.16 eV). Charge transport of these materials was investigated along with their morphological and microstructural studies. The fused planar aromatic structure having a five-membered ring, which is known to exhibit anti-aromaticity character, was combined with a strong EWG at the molecular termini to further lower the LUMO level. As a representative example, dithiarubicene which is an analog of rubicene with a high electron affinity. The effect of multiply cyano substituents (BisDCNE, BisTCNE and TCNQE) on OFET behavior was studied by Tsukamoto *et al*[93]. . The LUMO/HOMO energy levels measured by cyclic voltammetry are −3.97/−5.69 eV for BisDCNE, −4.23/−5.99 eV for BisTCNE, −4.20/−5.62 eV for TCNQE, respectively. BisTCNE exhibits both a deeper LUMO/HOMO

energy levels than TCNQE, and BisDCNE. Incorporation of three cyano units at the end of dithiarubicene core, led to a slightly decrease of both LUMO and HOMO of BisTCNE owing to the electron-withdrawing capacity of the cyano. OFET devices based on BisTCNE exhibit a better performance than those based on TCNQE. The optimum mobility of 0.055 $cm^2\ V^{-1}\ s^{-1}$ was demonstrated for BisTCNE. Ren and coworkers designed and synthetized a new molecule QDPPBTT featuring extremely low LUMO levels (-4.37 eV) [94]. DPP was incorporated without alkyl chain substitution to enhance the hydrogen bonding of DPP and better crystallinity. QDPPBTT-based OFET materials show promising electron mobility (0.13 $cm^2\ V^{-1}\ s^{-1}$).

Incorporation of fluorine atoms into the quinoid system resulted in FTQ1, FTQ2, and FTQ-3 (Figure 19) [95]. It was found that the HOMO/LUMO levels for fluorinated molecules were much lower than those of non-fluorinated analogues. When we compare fluorinated versus non-fluorinated analogues a down shift of the LUMO position by 0.2 eV was observed. The fluorinated terthiophene FTQ-2 adopts slipped π-π stacking. Furthermore, the fluorine substitution locks the planar conformation through the non-covalent bonding interaction of F and S. FTQ-3 annealed at 130°C exhibited the highest mobility among the three. Quinoidal oligothiophenes (QBDT and QTBDT-3H) have been developed by Lin *et al.*[96]. The LUMO levels of the two molecules are very close to each other. Increasing the conjugation length by adding one thiophene ring from QBDT to QTBDT-3H enhances the diradical character. Spin-coated films of QTBDT-3H and QBDT in OFET devices exhibited ambipolar transport behavior for QTBDT-3H and unipolar transport property for QBDT.

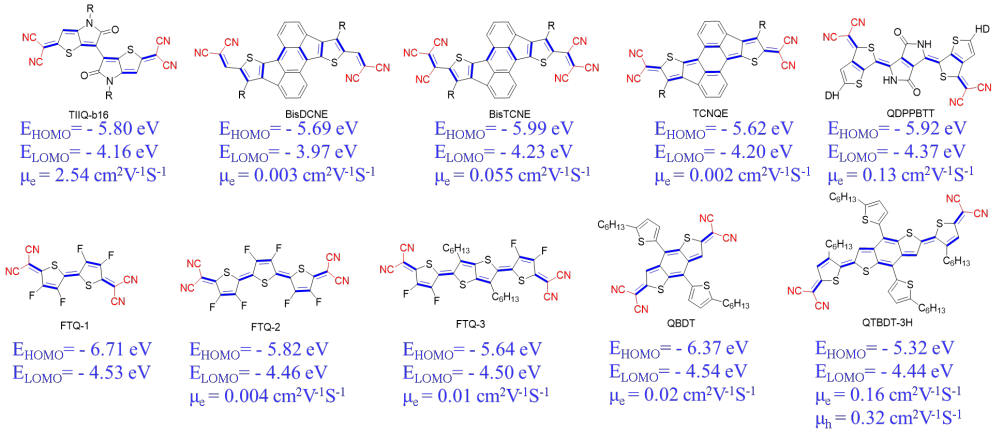

Figure 19. Example of molecular materials, based on dicyanomethylene end-capped OSCs for OFET application.

4.1.2. OFET performance of polymers developed as n-type channel materials

Thieno-quinoidal systems with oxindole group as the end group have proven to be excellent electron-deficient building blocks. Additionally, the outer benzene ring of the oxindole offers an excellent opportunity to further extend the conjugation length, via introduction of bromine atom and subsequent polymerisation by traditional palladium-catalyzed polycondensation. Deng and co-workers first reported the n-type quinoidal polymers (P1, Figure 15) [73]. These materials exhibited a moderate electron mobility (Table 3);. Later they reported the synthesis of two other polymers (P2, P3), with lower LUMO energy levels, suggesting that they have a lower barrier to electron injection in OFET. The electron mobility μ_e was further enhanced for OFET device due to more ordered films of P2. However, P3 showed much lower performance due to its amorphous film and poorer crystallinity. Replacing quinoidal bithiophene with quinoidal thienothiophene yielded polymer P6, with mobility of 0.45 $cm^2\ V^{-1}\ s^{-1}$ and air stability in OFETs, while P4 performed the worst, with maximum mobility of merely 0.004 $cm^2\ V^{-1}\ s^{-1}$.[56]

N-type OSC-materials are less developed than their p-type counterpart, due to their instability in air as well as their low electron mobility. So, design of n-type OSC materials with high electron mobility is an emerging field. Although, high performance OFETs device relies on not only the properties of n-type OSC active layer, but also the dielectrics and device processing techniques. An ideal n-type OSC semiconductors with high electron mobility and good stability in air should have a planar molecular structure with short intermolecular stacking distances. In addition, they should possess a deep LUMO (<-4.0 eV) to inhibit air oxidation, thus resulting in excellent ambient stability.

Table 3. OFET performance of polymers used in transistor applications (n-type).

Marerials	λmax (nm)	E_g^{opt} (eV)	E_{HOMO} (eV)	E_{LUMO} (eV)	OFET structure	μ_e ($cm^2/V{\cdot}s$)	Measured environment
P1	710	1.42	-5.92	-3.98	BGBC	0.14	N_2
P2	765	1.43	-5.78	-4.09	BGBC	0.18	N_2
P3	740	1.62	-5.99	-4.18	BGBC	0.016	N_2
P4	740	1.48	-6.00	-4.04	TGBC	0.004	air
P5	751	1.47	-5.95	-4.03	TGBC	0.38	air
P6	758	1.43	-5.91	-4.04	TGBC	0.45	air

4.1.3. OFET devices performance of polymers used in transistor applications (p-type and ambipolar)

P11-P13 were synthesized by Stille polymerization reaction (Figure 15). Among them, P11 exhibits the highest hole mobility under optimized conditions of processing with an annealing temperature of 300 ℃ (Table 4). Nevertheless, the performance is still relatively low compared to that of quinoidal materials. The insertion of fluorine atoms of oxindole ring in P16 has good impact on the coplanarity of the polymer chains with the best mobility up to 2.70 $cm^2\ V^{-1}\ s^{-1}$. Huang *et al*. investigated P18 with reversible structure between aromatic, open-shell, and quinoidal, closed-shell, forms. [97]. Hence, the energy level of LUMO of P18 has been lowered by 0.27 eV when compared to that of isoindigo analogue. The best OFET performance was achieved when the thin film was annealed at 300 °C. Using similar design strategy, Kim *et al* recently developed novel conjugated polymers P19 and P20 by incorporating quinoid moieties with different conjugation lengths units. These copolymers exhibit close- and open-shell biradical character depending on their quinoidal moiety[98]. The longer conjugation length results in the increased properties of diradical character, open-shell structure, of both monomer and the resulting copolymer. On the other hand, a smaller conjugation length of the quinoidal core maintains a closed-shell quinoid structure, the resulting copolymer exhibits a high backbone coplanarity and a strong intermolecular interaction. These characteristics are beneficial for charge transport. The optimum of OFET devices performance for P21 and P22 occurred after annealing at 250°C with a hole and an electron mobilities of 4.82 and 1.11 $cm^2\ V^{-1}\ s^{-1}$ and 8.09 and 0.74 $cm^2\ V^{-1}\ s^{-1}$, respectively. Hwang and coworkers synthesized quinoidal copolymer (P23), which has a quinoidal indophenine unit linked with a vinylene unit [99]. Introducing a vinylene link between the two indophenine units induces a highly coplanar. Ambipolar charge transport behaviors were identified in OFET devices. The HOMO and LUMO energy were found to be −5.08 and −3.79 eV, respectively. A further enhancement of the open-shell character of the conjugated copolymer with ambipolar semiconducting behavior was successfully achieved [100]. P24, exhibits an ambipolar charge-transport behavior in OFET devices (Table 4), however, the six isomers could not be successfully isolated[100].

In summary, this section highlights different synthetic strategies utilized in recent years, to develop novel quinoidal molecules and their use as a useful building block to produce novel polymers with high-spin characteristics, tunable optoelectronic properties, ambipolar and n-type semiconducting property.

Table 4. OFET device performance of polymers used in transistor applications (p-type).

Polymers	E_{HOMO} (eV)	E_{LUMO} (eV)	OFET structure	μ_h ($cm^2/V{\cdot}s$)	μ_e ($cm^2/V{\cdot}s$)	Measured environment
P7	-4.59	-3.63	TGBC	0.12		N_2
P8	-5.14	-3.62	TGBC	0.024	0.049	N_2
P9	-5.17	-3.58	TGBC	0.11	0.0014	N_2
P10	-5.17	-3.70	TGBC	0.017	0.00092	N_2
P11	-4.58	-3.43	TGBC	0.043		N_2
P12	-4.52	-3.36	TGBC	0.018		N_2
P13	-4.50	-3.32	TGBC	0.007		N_2
P14	-5.31	-3.95	TGBC	0.10		N_2
P15	-5.35	-3.92	TGBC	0.91		N_2
P16	-5.43	-3.97	TGBC	2.70		N_2
P17	-5.32	-3.92	TGBC	1.35		N_2
P18	-5.19	-3.63	BGTC	0.13		N_2
P19	-5.22	-3.43	TGBC	2.40	0.056	N_2
P20	-5.04	-3.65	TGBC	0.055	0.0015	N_2
P21	-5.24	-3.56	TGBC	4.82	1.11	N_2
P22	-5.11	-3.55	TGBC	8.09	0.74	N_2
P23	-5.08	-3.79	TGBC	0.52	0.53	N_2
P24	-5.03	-3.74	TGBC	0.35	0.46	N_2

4.2. Organic diradical TE materials

As noted during the introduction, the developments of TE-materials are very attractive from the point of view of achieving more efficient devices for energy harvesting. Both p-type and n-type materials are demanded in the advancement of the TE field. PEDOT:PSS is a benchmark p-type conducting polymer for TE applications, with a promising power factor of 47 $\mu W\ m^{-1}\ K^{-2}$ and higher electrical conductivity of 900 $S\ cm^{-1}$ [101]. In contrast, very few n-type polymer TE materials exhibited a moderate TE property. For instance, few reported materials can exhibit a conductivity higher than 90 $S\ cm^{-1}$ for N doped conjugated polymer based thiophene-fused benzodifurandione and good power factor of 106 $mW\ m^{-1}\ K^{-2}$ for doped copolymer[102]. There are many recent reviews covering the materials design [11, 103], n-type doping techniques [104].

The reason why n-type TE materials are less developed lies in the lack of materials with deeper LUMO levels for efficient electron injection, stable charge transport as well as an efficient n-type-doping process. N-doping of OSCs is extremely challenging because of the lack of OSC with deep LUMO (−4.7 eV) to effectively stabilize n-doping under ambient conditions. Recently many works have explored n-doping OSCs using various organic and inorganic salts, and pointed out the air-stability issue of doped materials. For instance, Katz *et al*. reported air-stable n-doped ClBDPPV with low LUMO energy of −4.3 eV (Figure 20). The electrical conductivity dropped by 50% within 24 h[105]. To overcome this limitation and generate materials with improved stability, diradicaloid materials with a deeper LUMO energy, represent an attractive approach. Yuan and coworkers found that diradical character and deep LUMO are favorable for stable and excellent thermoelectric performance[106].2DQTT provided the best compromise between stability and enhanced electrical performance. The substitution of Se for S is of assistance in changing the electronic properties of the system, due to the strong intermolecular Se···Se interactions and high polarizability of Se [107].

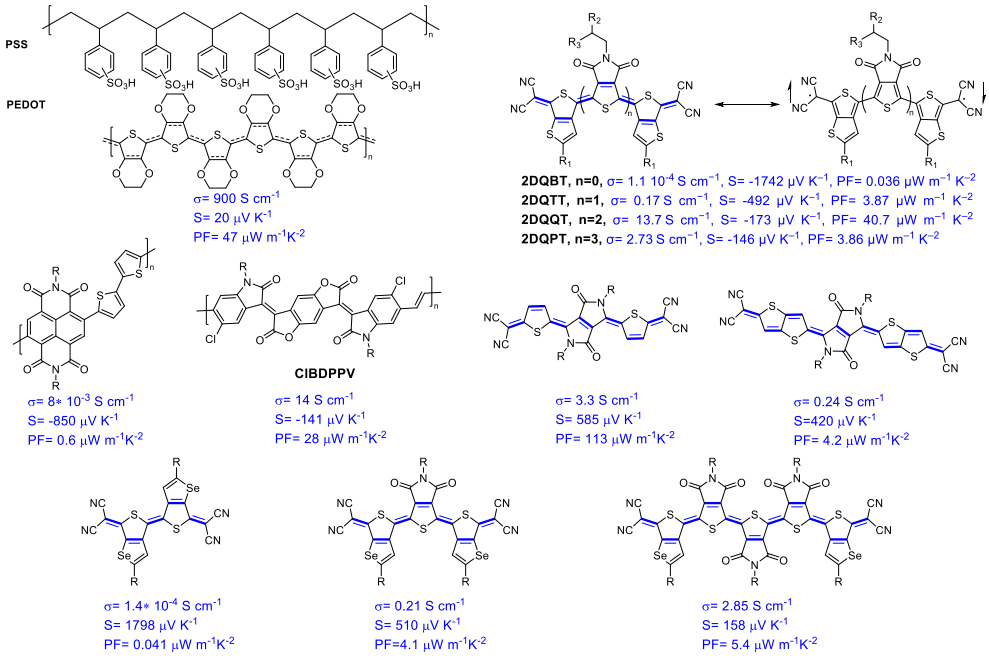

Figure 20. Top: Chemical structure of PEDOT:PSS, resonance structures and diradical dicyanomethylene end-capped oligothiophene; Bottom: Chemical structures of the most performing p-, n-type OSCs alongside with diradical materials developed for TE application.

4.3. Quinoidal semiconducting materials for photovoltaic applications

Quinoidal π-conjugated materials show outstanding optoelectronic properties in terms of a low band-gap with high absorption coefficients and remarkable charge-transport properties. Despite these features they are less investigated in photovoltaic applications. In contrast to aromatic forms, the optical band-gap of quinoidal form materials allows readily adjusting to obtain near-infrared light. Nonetheless, the main challenge in achieving efficient organic solar cells is obtaining high crystallinity. This prevents their use in photovoltaic devices and there are only few reports on this filed. For instance, Ren *et al* designed dithienoindophenine derivatives (μ_h, 0.22 $cm^2V^{-1}s^{-1}$) with suitable HOMO/LUMO (DTIP-I and DTIP-o in Figure 21). DTIP-o exhibits a better PCE of 4.07 % [57]. Another application of quinoidal materials in photovoltaic is their use as non-fullerene materials. Materials with fused forms with strong EWGs are promising acceptor materials for organic photovoltaics. Indacenodithiophene-based small molecular acceptor (ITIC) is an archetype n-type OSC and possesses a broad and strong absorption spectrum. This non-fullerene acceptor has been used in device reaching up to 12% in PCE[10]. Replacing the phenyl ring of the dicyanomethylene-indanone moiety with thiophene ring enhances the quinoidal character, which reduces the optical band-gap and enhances the near-IR absorptivity[108]. The maximum PCE and average PCE for ITCT were 11.27 % and 10.99 %, respectively.

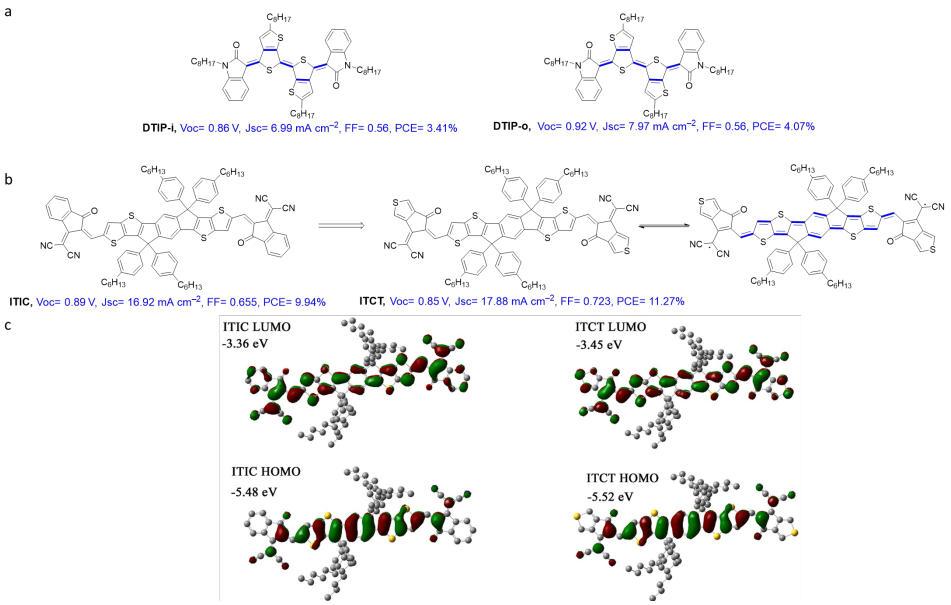

Figure 21. (a) Molecular structures of quinoidal DTIP-i and DTIP-o; (b) Molecular structures of ITIC and ITCT; (c) LUMO and HOMO energy levels distributions. Reproduced with the permission from ref[108].

5. Conclusions

In this review, we summarized the recent state-of-the-art progress and some guideline for the design of quinoidal organic semiconducting materials. Over past decade, high-performance n-type and ambipolar conjugated quinoidal systems have been extensively investigated. Indophenine-based structures showed a remarkably high electron and hole mobilities. Different synthetic strategies to improve the yield, reaction scale, regioselectivity and product functionality of indophenine dyes, have been discussed. The indophenine reaction simultaneously produces quinoidal compounds of different bridging lengths and contains multiple isomers, which greatly limits the yield and purity of the material. The primary problem to be solved for research in this field is the separation of mixed isomers, the presence of which results in an intricate NMR spectrum and the complexity of analyzing the quantitative proportions of each isomer. The presence of isomers is correlated with the performance of the device. We believe that the separation of materials with only one and two bridging groups is facilitated by exploiting the difference in solubility of small molecular materials of different lengths in various organic solvents. By engineering the π-bridge group, the intermolecular interactions can be used to drive the formation of one isomer. Few materials based on indophenin indophenine showed good performance in terms of hole mobility up to 8.09 $cm^2V^{-1}s^{-1}$, but most materials exhibit a mobility of 1 $cm^2V^{-1}s^{-1}$. The electron mobility was shown to be worse than the hole mobility, which is related to the electron donating nature of the thiophene or EDOT rings contained in their structures. Designing unipolar high electron mobility materials or ambipolar materials with balanced ambipolar properties remain a challenge for organic chemists. Quinoidal structures are among the emerging building blocks for constructing high performance n-type and ambipolar semiconducting materials. Rational structural design strategies are an efficient approach to enhance the electrical and optical properties, for instance, the introduction of strong electron-withdrawing groups, i.e., fluorine and chlorine atoms, into the oxindole ring, which does not affect the selectivity of the reaction, single isomer formation, however enhance the planarity of the material, while significantly lowering the LUMO energy level of the material and subsequently enhance its electron transport ability and stability in air. Another possible direction in this field comes from the processing of devices, which often require the use of chlorinated solvents such as chloroform and chlorobenzene due to the poor solubility of indophenine based materials which increases

production costs and environmental pollution. So by engineering of the side chains of the materials, for instance the introduction of more soluble chains on oxindole rin, facilitates the preparation of intrinsically highly soluble materials, making the quinoloidal molecules more soluble in non-halogenated organic solvents, which facilitates the fabrication of devices by solution processes. On the other hand, most of the reported polymeric materials based on indophenine use Stille coupling reactions which involves organotin intermediates that have a potential environmental impact. We believed that the use of C-H activated cross-coupling and metal-free polymerization routes to π-conjugated polymers will inspire new research directions in in this field. The studies of different molecular structures of conjugated quinoidal materials, with variable termini and π-conjugated core are helpful to understand the structure-property relationships. The effects of various end-groups, π-conjugated core, conjugated backbones, and side chains, on the OFET performance are able to provide guides for synthesizing new generations of quinoidal or diradical materials with tunable optoelectronic properties and more outstanding charge carrier mobility of up 8.09 $cm^2 V^{-1} s^{-1}$ in OFET devices.

Author Contributions: Abderrahim Yassar suggested this review and organized all sections. Both authors contributed equally to write and review the manuscript.

Funding: This research was funded by ANR-16-CE07-0024 (GATE). Shiwei. Ren thanks the China Scholarship Council for a PhD fellowship (No.201808070090) and the fellowship of China Postdoctoral Science Foundation（No.2022TQ0399).

Conflicts of Interest: The authors declare no conflict of interest.

References

(1) Takimiya, K.; Nakano, M. Thiophene-Fused Naphthalene Diimides: New Building Blocks for Electron Deficient π-Functional Materials. *Bulletin of the Chemical Society of Japan* **2018**, *91* (1), 121-140. DOI: 10.1246/bcsj.20170298.

(2) Fan, Y. W.; Liu, J.; Hu, W. P.; Liu, Y. Q.; Jiang, L. The effect of thickness on the optoelectronic properties of organic field-effect transistors: towards molecular crystals at monolayer limit. *Journal of Materials Chemistry C* **2020**, *8* (38), 13154-13168. DOI: 10.1039/d0tc03193c.

(3) Yuvaraja, S.; Nawaz, A.; Liu, Q.; Dubal, D.; Surya, S. G.; Salama, K. N.; Sonar, P. Organic field-effect transistor-based flexible sensors. *Chemical Society Reviews* **2020**, *49* (11), 3423-3460. DOI: 10.1039/c9cs00811j.

(4) Li, H.; Brédas, J.-L. Developing molecular-level models for organic field-effect transistors. *National Science Review* **2020**. DOI: 10.1093/nsr/nwaa167 (acccessed 3/31/2021).

(5) Sirringhaus, H. 25th Anniversary Article: Organic Field-Effect Transistors: The Path Beyond Amorphous Silicon. *Advanced Materials* **2014**, *26* (9), 1319-1335. DOI: 10.1002/adma.201304346.

(6) Gunes, S.; Neugebauer, H.; Sariciftci, N. S. Conjugated polymer-based organic solar cells. *Chemical Reviews* **2007**, *107* (4), 1324-1338. DOI: 10.1021/cr050149z.

(7) Hou, J. H.; Inganas, O.; Friend, R. H.; Gao, F. Organic solar cells based on non-fullerene acceptors. *Nature Materials* **2018**, *17* (2), 119-128. DOI: 10.1038/nmat5063.

(8) Choi, J.; Gordon, M. P.; Yuan, P.; Kang, H.; Zaia, E. W.; Urban, J. J. CHAPTER 1 Introduction. In *Organic Thermoelectric Materials*, The Royal Society of Chemistry, 2020; pp 1-20.

(9) Russ, B.; Glaudell, A.; Urban, J. J.; Chabinyc, M. L.; Segalman, R. A. Organic thermoelectric materials for energy harvesting and temperature control. *Nature Reviews Materials* **2016**, *1* (10), 16050. DOI: 10.1038/natrevmats.2016.50.

(10) Zhang, J.; Tan, H. S.; Guo, X.; Facchetti, A.; Yan, H. Material insights and challenges for non-fullerene organic solar cells based on small molecular acceptors. *Nature Energy* **2018**, *3* (9), 720-731. DOI: 10.1038/s41560-018-0181-5.

(11) Zhang, C.; Zhu, X. Z. n-Type Quinoidal Oligothiophene-Based Semiconductors for Thin-Film Transistors and Thermoelectrics. *Advanced Functional Materials* **2020**, *30* (31). DOI: 10.1002/adfm.202000765.

(12) Sun, Y. L.; Guo, Y. L.; Liu, Y. Q. Design and synthesis of high performance pi-conjugated materials through antiaromaticity and quinoid strategy for organic field-effect transistors. *Materials Science & Engineering R-Reports* **2019**, *136*, 13-26. DOI: 10.1016/j.mser.2018.10.003.

(13) Casado, J. Para-Quinodimethanes: A Unified Review of the Quinoidal-Versus-Aromatic Competition and its Implications. *Topics in Current Chemistry* **2017**, *375* (4). DOI: 10.1007/s41061-017-0163-2.

(14) Huang, J. Y.; Yu, G. Recent progress in quinoidal semiconducting polymers: structural evolution and insight. *Materials Chemistry Frontiers* **2021**, *5* (1), 76-96. DOI: 10.1039/d0qm00509f.

(15) Li, G.; Matsuno, T.; Han, Y.; Wu, S.; Zou, Y.; Jiang, Q.; Isobe, H.; Wu, J. Fused Quinoidal Dithiophene-Based Helicenes: Synthesis by Intramolecular Radical–Radical Coupling Reactions and Dynamics of Interconversion of Enantiomers. *Angewandte Chemie International Edition* **2021**, *60* (18), 10326-10333. DOI: https://doi.org/10.1002/anie.202100606.

(16) Wang, J.; Xu, X.; Phan, H.; Herng, T. S.; Gopalakrishna, T. Y.; Li, G.; Ding, J.; Wu, J. Stable Oxindolyl-Based Analogues of Chichibabin's and Müller's Hydrocarbons. *Angewandte Chemie International Edition* **2017**, *56* (45), 14154-14158. DOI: https://doi.org/10.1002/anie.201708612.

(17) Acker, D. S.; Harder, R. J.; Hertler, W. R.; Mahler, W.; Melby, L. R.; Benson, R. E.; Mochel, W. E. 7,7,8,8-TETRACYANOQUINODIMETHANE AND ITS ELECTRICALLY CONDUCTING ANION-RADICAL DERIVATIVES. *Journal of the American Chemical Society* **1960**, *82* (24), 6408-6409. DOI: 10.1021/ja01509a052.

(18) Torrance, J. B. The difference between metallic and insulating salts of tetracyanoquinodimethone (TCNQ): how to design an organic metal. *Accounts of Chemical Research* **1979**, *12* (3), 79-86. DOI: 10.1021/ar50135a001.

(19) Liu, E.-C.; Topczewski, J. J. Gram-Scale Synthesis of 2,5-Difluoro-7,7,8,8-tetracyanoquinodimethane (F2-TCNQ). *The Journal of Organic Chemistry* **2020**, *85* (6), 4560-4564. DOI: 10.1021/acs.joc.0c00053.

(20) Uno, M.; Seto, K.; Takahashi, S. A new method of synthesis of arylmalononitriles catalysed by a palladium complex. *Journal of the Chemical Society, Chemical Communications* **1984**, (14), 932-933, 10.1039/C39840000932. DOI: 10.1039/C39840000932.

(21) Takahashi, K.; Tarutani, S. Novel electron acceptors for organic conductors: 1,2-bis(p-benzoquino)-3-[2-(dicyanomethylene)-2,5-thienoquino]cyclopropane derivatives. *Journal of the Chemical Society, Chemical Communications* **1994**, (4), 519-520, 10.1039/C39940000519. DOI: 10.1039/C39940000519.

(22) Uno, M.; Seto, K.; Masuda, M.; Ueda, W.; Takahashi, S. A new route to phenylenedimalononitrile and the analogues using palladium-catalyzed carbon-carbon bond formation. *Tetrahedron Letters* **1985**, *26* (12), 1553-1556. DOI: https://doi.org/10.1016/S0040-4039(00)98550-2.

(23) Yamaguchi, S.; Nagareda, K.; Hanafusa, T. Synthesis of 1,2,3,6,7,8-hexahydro-10,10,11,11-tetracyano-4,9-pyrenoquinodimethane. *Synthetic Metals* **1989**, *30* (3), 401-402. DOI: https://doi.org/10.1016/0379-6779(89)90664-4.

(24) Martín, N.; Segura, J. L.; Seoane, C. Design and synthesis of TCNQ and DCNQI type electron acceptor molecules as precursors for 'organic metals'. *Journal of Materials Chemistry* **1997**, *7* (9), 1661-1676, 10.1039/A702314F. DOI: 10.1039/A702314F.

(25) Takimiya, K.; Kawabata, K. Thienoquinoidal System: Promising Molecular Architecture for Optoelectronic Applications. *Journal of Synthetic Organic Chemistry, Japan* **2018**, *76* (11), 1176-1184. DOI: 10.5059/yukigoseikyokaishi.76.1176.

(26) Zhang, C.; Zhu, X. n-Type Quinoidal Oligothiophene-Based Semiconductors for Thin-Film Transistors and Thermoelectrics. *Advanced Functional Materials* **2020**, *30* (31), 2000765. DOI: https://doi.org/10.1002/adfm.202000765.

(27) Lu, J.; Dadvand, A.; Chu, T.-y.; Movileanu, R.; Baribeau, J.-M.; Ding, J.; Tao, Y. Inkjet-printed unipolar n-type transistors on polymer substrates based on dicyanomethylene-substituted diketopyrrolopyrrole quinoidal compounds. *Organic Electronics* **2018**, *63*, 267-275. DOI: https://doi.org/10.1016/j.orgel.2018.09.035.

(28) Qiao, Y.; Guo, Y.; Yu, C.; Zhang, F.; Xu, W.; Liu, Y.; Zhu, D. Diketopyrrolopyrrole-Containing Quinoidal Small Molecules for High-Performance, Air-Stable, and Solution-Processable n-Channel Organic Field-Effect Transistors. *Journal of the American Chemical Society* **2012**, *134* (9), 4084-4087. DOI: 10.1021/ja3003183.

(29) Jiang, H.; Oniwa, K.; Xu, Z.; Bao, M.; Yamamoto, Y.; Jin, T. Synthesis and Properties of Dicyanomethylene-Endcapped Thienopyrrole-Based Quinoidal S,N-Heteroacenes. *Bulletin of the Chemical Society of Japan* **2017**, *90* (7), 789-797. DOI: 10.1246/bcsj.20170083.

(30) Joseph, V.; Yu, C.-H.; Lin, C.-C.; Lien, W.-C.; Tsai, H.-C.; Chen, C.-S.; Torimtubun, A. A. A.; Velusamy, A.; Huang, P.-Y.; Lee, G.-H.; et al. Quinoidal thioalkyl-substituted bithiophene small molecule semiconductors for n-type organic field effect transistors. *Journal of Materials Chemistry C* **2020**, *8* (43), 15450-15458, 10.1039/D0TC03808C. DOI: 10.1039/D0TC03808C.

(31) Vegiraju, S.; Amelenan Torimtubun, A. A.; Lin, P.-S.; Tsai, H.-C.; Lien, W.-C.; Chen, C.-S.; He, G.-Y.; Lin, C.-Y.; Zheng, D.; Huang, Y.-F.; et al. Solution-Processable Quinoidal Dithioalkylterthiophene-Based Small Molecules Pseudo-Pentathienoacenes via an Intramolecular S···S Lock for High-Performance n-Type Organic Field-Effect Transistors. *ACS Applied Materials & Interfaces* **2020**, *12* (22), 25081-25091. DOI: 10.1021/acsami.0c03477.

(32) Canesi, E. V.; Fazzi, D.; Colella, L.; Bertarelli, C.; Castiglioni, C. Tuning the Quinoid versus Biradicaloid Character of Thiophene-Based Heteroquaterphenoquinones by Means of Functional Groups. *Journal of the American Chemical Society* **2012**, *134* (46), 19070-19083. DOI: 10.1021/ja3072385.

(33) Badía-Domínguez, I.; Peña-Álvarez, M.; Wang, D.; Pérez Guardiola, A.; Vida, Y.; Rodríguez González, S.; López Navarrete, J. T.; Hernández Jolín, V.; Sancho García, J. C.; García Baonza, V.; et al. Dynamic Covalent Properties of a Novel Indolo[3,2-b]carbazole Diradical. *Chemistry – A European Journal* **2021**, *27* (17), 5509-5520. DOI: https://doi.org/10.1002/chem.202005211.

(34) Yamamoto, K.; Jinnai, S.; Takehara, T.; Suzuki, T.; Ie, Y. Quinoidal Oligothiophenes Having Full Benzene Annelation: Synthesis, Properties, Structures, and Acceptor Application in Organic Photovoltaics. *Organic Letters* **2020**, *22* (2), 547-551. DOI: 10.1021/acs.orglett.9b04314.

(35) Yamamoto, K.; Ie, Y.; Nitani, M.; Tohnai, N.; Kakiuchi, F.; Zhang, K.; Pisula, W.; Asadi, K.; Blom, P. W. M.; Aso, Y. Oligothiophene quinoids containing a benzo[c]thiophene unit for the stabilization of the quinoidal electronic structure. *Journal of Materials Chemistry C* **2018**, *6* (28), 7493-7500, 10.1039/C8TC01802B. DOI: 10.1039/C8TC01802B.

(36) Velusamy, A.; Yu, C.-H.; Afraj, S. N.; Lin, C.-C.; Lo, W.-Y.; Yeh, C.-J.; Wu, Y.-W.; Hsieh, H.-C.; Chen, J.; Lee, G.-H.; et al. Thienoisoindigo (TII)-Based Quinoidal Small Molecules for High-Performance n-Type Organic Field Effect Transistors. *Advanced Science* **2021**, *8* (1), 2002930. DOI: https://doi.org/10.1002/advs.202002930.

(37) Du, T.; Gao, R.; Deng, Y.; Wang, C.; Zhou, Q.; Geng, Y. Indandione-Terminated Quinoids: Facile Synthesis by Alkoxide-Mediated Rearrangement Reaction and Semiconducting Properties. *Angewandte Chemie International Edition* **2020**, *59* (1), 221-225. DOI: https://doi.org/10.1002/anie.201911530.

(38) Wang, C.; Du, T.; Liang, Z.; Zhu, J.; Ren, J.; Deng, Y. Synthesis of low-bandgap small molecules by extending the π-conjugation of the termini in quinoidal compounds. *Journal of Materials Chemistry C* **2021**, *9* (6), 2054-2062, 10.1039/D0TC04962J. DOI: 10.1039/D0TC04962J.

(39) Yang, M.; Du, T.; Zhao, X.; Huang, X.; Pan, L.; Pang, S.; Tang, H.; Peng, Z.; Ye, L.; Deng, Y.; et al. Low-bandgap conjugated polymers based on benzodipyrrolidone with reliable unipolar electron mobility exceeding 1 cm2 V−1 s−1. *Science China Chemistry* **2021**, *64* (7), 1219-1227. DOI: 10.1007/s11426-021-9991-0.

(40) Montgomery, L. K.; Huffman, J. C.; Jurczak, E. A.; Grendze, M. P. The molecular structures of Thiele's and Chichibabin's hydrocarbons. *Journal of the American Chemical Society* **1986**, *108* (19), 6004-6011. DOI: 10.1021/ja00279a056.

(41) Ishii, A.; Horikawa, Y.; Takaki, I.; Shibata, J.; Nakayama, J.; Hoshino, M. Preparation of 2,5-bis(diarylmethylene)-2,5-dihydrothiophenes and their furan, selenophene, and N-methylpyrrole analogs. *Tetrahedron Letters* **1991**, *32* (34), 4313-4316. DOI: https://doi.org/10.1016/S0040-4039(00)92158-0.

(42) Kawase, T.; Ueno, N.; Oda, M. Perthienyl analogues of chichibabin's hydrocarbon. A new stable, highly amphoteric multistage redox system with low oxidation potentials. *Tetrahedron Letters* **1992**, *33* (37), 5405-5408. DOI: https://doi.org/10.1016/S0040-4039(00)79106-4.

(43) Takeda, T.; Akutagawa, T. Preparation, Structure, and Redox Behavior of Bis(diarylmethylene)dihydrothiophene and Its π-Extended Analogues. *The Journal of Organic Chemistry* **2015**, *80* (4), 2455-2461. DOI: 10.1021/acs.joc.5b00021.

(44) Mazaki, Y.; Murata, S.; Kobayashi, K. Thermal and photochemical formation of quinonoid derivatives of condensed polythiophenes and their spectral properties. *Tetrahedron Letters* **1991**, *32* (34), 4367-4370. DOI: https://doi.org/10.1016/S0040-4039(00)92172-5.

(45) Wang, K.; Li, Z.; Huang, J.; Wang, T.; Gao, J.; Gao, Y.; Wang, S.; He, S.; Lv, A.; Wang, M. Design and synthesis of two conjugated semiconductors containing quinoidal cyclopentadithiophene core. *Dyes and Pigments* **2021**, *190*, 109336. DOI: https://doi.org/10.1016/j.dyepig.2021.109336.

(46) Jiménez, V. G.; Mayorga-Burrezo, P.; Blanco, V.; Lloveras, V.; Gómez-García, C. J.; Šolomek, T.; Cuerva, J. M.; Veciana, J.; Campaña, A. G. Dibenzocycloheptatriene as end-group of Thiele and tetrabenzo-Chichibabin hydrocarbons. *Chemical Communications* **2020**, *56* (84), 12813-12816, 10.1039/D0CC04489J. DOI: 10.1039/D0CC04489J.

(47) Baeyer, A. Untersuchungen über die Gruppe des Indigblaus. *Berichte der deutschen chemischen Gesellschaft* **1879**, *12* (2), 1309-1319. DOI: https://doi.org/10.1002/cber.18790120221.

(48) Meyer, V. Ueber Benzole verschiedenen Ursprungs. *Berichte der deutschen chemischen Gesellschaft* **1882**, *15* (2), 2893-2894. DOI: https://doi.org/10.1002/cber.188201502279.

(49) Tormos, G. V.; Belmore, K. A.; Cava, M. P. The indophenine reaction revisited. Properties of a soluble dialkyl derivative. *Journal of the American Chemical Society* **1993**, *115* (24), 11512-11515. DOI: 10.1021/ja00077a057.

(50) Hwang, H.; Khim, D.; Yun, J. M.; Jung, E.; Jang, S. Y.; Jang, Y. H.; Noh, Y. Y.; Kim, D. Y. Quinoidal molecules as a new class of ambipolar semiconductor originating from amphoteric redox behavior. *Advanced Functional Materials* **2015**, *25* (7), 1146-1156. DOI: 10.1002/adfm.201402758.

(51) Kim, Y.; Hwang, H.; Kim, N. K.; Hwang, K.; Park, J. J.; Shin, G. I.; Kim, D. Y. pi-Conjugated Polymers Incorporating a Novel Planar Quinoid Building Block with Extended Delocalization and High Charge Carrier Mobility. *Adv Mater* **2018**, *30* (22), 1706557. DOI: 10.1002/adma.201706557.

(52) Kim, Y.; Kim, Y. J.; Kim, Y. A.; Jung, E.; Mok, Y.; Kim, K.; Hwang, H.; Park, J. J.; Kim, M. G.; Mathur, S.; et al. Open-Shell and Closed-Shell Quinoid-Aromatic Conjugated Polymers: Unusual Spin Magnetic and High Charge Transport Properties. *ACS Appl Mater Interfaces* **2021**, *13* (2), 2887-2898. DOI: 10.1021/acsami.0c15893.

(53) Jiang, H.; Hu, Q.; Cai, J.; Cui, Z.; Zheng, J.; Chen, W. Synthesis and dyeing properties of indophenine dyes for polyester fabrics. *Dyes and Pigments* **2019**, *166*, 130-139. DOI: https://doi.org/10.1016/j.dyepig.2019.03.025.

(54) Cai, J.; Jiang, H.; Chen, W.; Cui, Z. Design, synthesis, characterization of water-soluble indophenine dyes and their application for dyeing of wool, silk and nylon fabrics. *Dyes and Pigments* **2020**, *179*. DOI: 10.1016/j.dyepig.2020.108385.

(55) Bhanvadia, V. J.; Choudhury, A.; Iyer, P. K.; Zade, S. S.; Patel, A. L. Constructing fused bis-isatins from pyrroloindoles using direct oxidation approach and re-visiting indophenine reaction. *Polymer* **2020**, *210*. DOI: 10.1016/j.polymer.2020.123032.

(56) Guo, K.; Wu, B.; Jiang, Y.; Wang, Z.; Liang, Z.; Li, Y.; Deng, Y.; Geng, Y. Synthesis of an isomerically pure thienoquinoid for unipolar n-type conjugated polymers: effect of backbone curvature on charge transport performance. *Journal of Materials Chemistry C* **2019**, *7* (33), 10352-10359, 10.1039/C9TC03556G. DOI: 10.1039/C9TC03556G.

(57) Ren, L.; Fan, H.; Huang, D.; Yuan, D.; Di, C.-a.; Zhu, X. Dithienoindophenines: p-Type Semiconductors Designed by Quinoid Stabilization for Solar-Cell Applications. *Chemistry – A European Journal* **2016**, *22* (48), 17136-17140. DOI: 10.1002/chem.201603112.

(58) Ren, L.; Fan, H.; Huang, D.; Yuan, D.; Di, C. A.; Zhu, X. Dithienoindophenines: p-Type Semiconductors Designed by Quinoid Stabilization for Solar-Cell Applications. *Chemistry* **2016**, *22* (48), 17136-17140. DOI: 10.1002/chem.201603112.

(59) Deng, Y.; Sun, B.; He, Y.; Quinn, J.; Guo, C.; Li, Y. Thiophene - S, S - dioxidized Indophenine: A Quinoid - Type Building Block with High Electron Affinity for Constructing n - Type Polymer Semiconductors with Narrow Band Gaps. *Angewandte Chemie International Edition* **2016**, *55* (10), 3459-3462. DOI: 10.1002/anie.201508781.

(60) Deng, Y.; Quinn, J.; Sun, B.; He, Y.; Ellard, J.; Li, Y. Thiophene-S, S-dioxidized indophenine (IDTO) based donor–acceptor polymers for n-channel organic thin film transistors. *RSC advances* **2016**, *6* (41), 34849-34854. DOI: 10.1039/C6RA03221D.

(61) Hu, Q.; Jiang, H.; Cui, Z.; Chen, W. An insight into the effect of S, S-dioxided thiophene on the opto-physical/electro-chemical properties and light stability for indophenine derivatives. *Dyes and Pigments* **2020**, *173*, 107891. DOI: 10.1016/j.dyepig.2019.107891.

(62) Deng, Y.; Sun, B.; Quinn, J.; He, Y.; Ellard, J.; Guo, C.; Li, Y. Thiophene-S, S-dioxidized indophenines as high performance n-type organic semiconductors for thin film transistors. *RSC advances* **2016**, *6* (51), 45410-45418. DOI: 10.1039/C6RA06316K.

(63) Gao, R.; Wu, B.; Liang, Z.; Zhao, X.; Deng, Y.; Tian, H.; Geng, Y. Electronic properties modulation of tetraoxidothieno[3,2-b]thiophene-based quinoidal compounds by terminal fluorination. *Materials Chemistry Frontiers* **2020**, *4* (3), 891-898, 10.1039/C9QM00690G. DOI: 10.1039/C9QM00690G.

(64) Lin, L.; Wang, C.; Deng, Y.; Geng, Y. Isomerically Pure Oxindole-Terminated Quinoids for n-Type Organic Thin-Film Transistors Enabled by the Chlorination of Quinoidal Core. *Chemistry – A European Journal n/a* (n/a), e202203336. DOI: https://doi.org/10.1002/chem.202203336.

(65) Pappenfus, T. M.; Helmin, A. J.; Wilcox, W. D.; Severson, S. M.; Janzen, D. E. ProDOT-Assisted Isomerically Pure Indophenines. *The Journal of Organic Chemistry* **2019**, *84* (17), 11253-11257. DOI: 10.1021/acs.joc.9b01525.

(66) Hwang, K.; Lee, M.-H.; Kim, J.; Kim, Y.-J.; Kim, Y.; Hwang, H.; Kim, I.-B.; Kim, D.-Y. 3,4-Ethylenedioxythiophene-Based Isomer-Free Quinoidal Building Block and Conjugated Polymers for Organic Field-Effect Transistors. *Macromolecules* **2020**, *53* (6), 1977-1987. DOI: 10.1021/acs.macromol.9b02237.

(67) Kim, Y.; Choi, Y.; Hwang, H.; Kang, M.; Hwang, K.; Lee, M.-H.; Kim, D.-Y. Isomer-Free Quinoidal Conjugated Polymers with Different Core Lengths for Organic Field-Effect Transistors. *ACS Applied Polymer Materials* **2022**, *4* (11), 8520-8526. DOI: 10.1021/acsapm.2c01429.

(68) Choi, Y.; Kim, Y.; Moon, Y.; Kim, I.-B.; Hwang, H.; Kim, D.-Y. Significant alternation of molecular structures and properties in quinoidal conjugated polymers by chalcogen atom substitution. *Journal of Materials Chemistry C* **2022**, *10* (47), 17874-17885, 10.1039/D2TC04122G. DOI: 10.1039/D2TC04122G.

(69) Sun, Y.; Zhang, Y.; Ran, Y.; Shi, L.; Zhang, Q.; Chen, J.; Li, Q.; Guo, Y.; Liu, Y. Methoxylation of quinoidal bithiophene as a single regioisomer building block for narrow-bandgap conjugated polymers and high-performance organic field-effect transistors. *Journal of Materials Chemistry C* **2020**, 10.1039/D0TC02199G. DOI: 10.1039/D0TC02199G.

(70) Ren, S.; Habibi, A.; Ni, P.; Nahdi, H.; Bouanis, F. Z.; Bourcier, S.; Clavier, G.; Frigoli, M.; Yassar, A. Synthesis and characterization of solution-processed indophenine derivatives for function as a hole transport layer for perovskite solar cells. *Dyes and Pigments* **2023**, 111136. DOI: https://doi.org/10.1016/j.dyepig.2023.111136.

(71) Hu, Q.; Jiang, H.; Cui, Z.; Chen, W. An insight into the effect of S,S-dioxided thiophene on the opto-physical/electro-chemical properties and light stability for indophenine derivatives. *Dyes and Pigments* **2020**, *173*, 107891. DOI: https://doi.org/10.1016/j.dyepig.2019.107891.

(72) Raimundo, J.-M.; Blanchard, P.; Frère, P.; Mercier, N.; Ledoux-Rak, I.; Hierle, R.; Roncali, J. Push－pull chromophores based on 2,2′-bi(3,4-ethylenedioxythiophene) (BEDOT) π-conjugating spacer. *Tetrahedron Letters* **2001**, *42* (8), 1507-1510. DOI: https://doi.org/10.1016/S0040-4039(00)02317-0.

(73) Deng, Y.; Sun, B.; He, Y.; Quinn, J.; Guo, C.; Li, Y. Thiophene-S,S-dioxidized Indophenine: A Quinoid-Type Building Block with High Electron Affinity for Constructing n-Type Polymer Semiconductors with Narrow Band Gaps. *Angewandte Chemie International Edition* **2016**, *55* (10), 3459-3462. DOI: 10.1002/anie.201508781.

(74) Sun, Y.; Zhang, Y.; Ran, Y.; Shi, L.; Zhang, Q.; Chen, J.; Li, Q.; Guo, Y.; Liu, Y. Methoxylation of quinoidal bithiophene as a single regioisomer building block for narrow-bandgap conjugated polymers and high-performance organic field-effect transistors. *Journal of Materials Chemistry C* **2020**, *8* (43), 15168-15174, 10.1039/D0TC02199G. DOI: 10.1039/D0TC02199G.

(75) Zeng, Z.; Shi, X.; Chi, C.; López Navarrete, J. T.; Casado, J.; Wu, J. Pro-aromatic and anti-aromatic π-conjugated molecules: an irresistible wish to be diradicals. *Chemical Society Reviews* **2015**, *44* (18), 6578-6596, 10.1039/C5CS00051C. DOI: 10.1039/C5CS00051C.

(76) Dressler, J. J.; Haley, M. M. Learning how to fine-tune diradical properties by structure refinement. *Journal of Physical Organic Chemistry* **2020**, *33* (11), e4114. DOI: https://doi.org/10.1002/poc.4114.

(77) Das, S.; Wu, J. Polycyclic Hydrocarbons with an Open-Shell Ground State. *Physical Sciences Reviews* **2017**, *2*. DOI: 10.1515/psr-2016-0109.

(78) Jiang, Q.; Han, Y.; Zou, Y.; Phan, H.; Yuan, L.; Herng, T. S.; Ding, J.; Chi, C. S-shaped para-Quinodimethane-Embedded Double [6]Helicene and Its Charged Species Showing Open-Shell Diradical Character. *Chemistry – A European Journal* **2020**, *26* (67), 15613-15622. DOI: https://doi.org/10.1002/chem.202002952.

(79) Cheng Lee, J. J.; Dong, S.; Ong, A.; Han, Y.; Wu, J.; Chi, C. A Tetraindeno-Fused Bis(anthraoxa)quinodimethane with Nine Consecutively Fused Six-Membered Rings. *Organic Letters* **2021**, *23* (8), 3027-3031. DOI: 10.1021/acs.orglett.1c00705.

(80) Zhang, C.; Medina Rivero, S.; Liu, W.; Casanova, D.; Zhu, X.; Casado, J. Stable Cross-Conjugated Tetrathiophene Diradical. *Angewandte Chemie International Edition* **2019**, *58* (33), 11291-11295. DOI: https://doi.org/10.1002/anie.201904153.

(81) Shimizu, A.; Kishi, R.; Nakano, M.; Shiomi, D.; Sato, K.; Takui, T.; Hisaki, I.; Miyata, M.; Tobe, Y. Indeno[2,1-b]fluorene: A 20-π-Electron Hydrocarbon with Very Low-Energy Light Absorption. *Angewandte Chemie International Edition* **2013**, *52* (23), 6076-6079. DOI: https://doi.org/10.1002/anie.201302091.

(82) Ponce Ortiz, R.; Casado, J.; Hernández, V.; López Navarrete, J. T.; Viruela, P. M.; Ortí, E.; Takimiya, K.; Otsubo, T. On the Biradicaloid Nature of Long Quinoidal Oligothiophenes: Experimental Evidence Guided by Theoretical Studies. *Angewandte Chemie International Edition* **2007**, *46* (47), 9057-9061. DOI: https://doi.org/10.1002/anie.200703244.

(83) Kato, K.; Osuka, A. Platforms for Stable Carbon-Centered Radicals. *Angewandte Chemie International Edition* **2019**, *58* (27), 8978-8986. DOI: https://doi.org/10.1002/anie.201900307.

(84) Zafra, J. L.; Qiu, L.; Yanai, N.; Mori, T.; Nakano, M.; Alvarez, M. P.; Navarrete, J. T. L.; Gómez-García, C. J.; Kertesz, M.; Takimiya, K.; et al. Reversible Dimerization and Polymerization of a Janus Diradical To Produce Labile C−C Bonds and Large Chromic Effects. *Angewandte Chemie International Edition* **2016**, *55* (47), 14563-14568. DOI: https://doi.org/10.1002/anie.201605997.

(85) Morita, Y.; Suzuki, S.; Sato, K.; Takui, T. Synthetic organic spin chemistry for structurally well-defined open-shell graphene fragments. *Nature Chemistry* **2011**, *3* (3), 197-204. DOI: 10.1038/nchem.985.

(86) Shimizu, A.; Hirao, Y.; Matsumoto, K.; Kurata, H.; Kubo, T.; Uruichi, M.; Yakushi, K. Aromaticity and pi-bond covalency: prominent intermolecular covalent bonding interaction of a Kekule hydrocarbon with very significant singlet biradical character. *Chem Commun (Camb)* **2012**, *48* (45), 5629-5631. DOI: 10.1039/c2cc31955a.

(87) Shimizu, A.; Hirao, Y.; Matsumoto, K.; Kurata, H.; Kubo, T.; Uruichi, M.; Yakushi, K. Aromaticity and π-bond covalency: prominent intermolecular covalent bonding interaction of a Kekulé hydrocarbon with very significant singlet biradical character. *Chemical Communications* **2012**, *48* (45), 5629-5631, 10.1039/C2CC31955A. DOI: 10.1039/C2CC31955A.

(88) Abe, M. Diradicals. *Chemical Reviews* **2013**, *113* (9), 7011-7088. DOI: 10.1021/cr400056a.

(89) Tian, Y.; Uchida, K.; Kurata, H.; Hirao, Y.; Nishiuchi, T.; Kubo, T. Design and Synthesis of New Stable Fluorenyl-Based Radicals. *Journal of the American Chemical Society* **2014**, *136* (36), 12784-12793. DOI: 10.1021/ja507005c.

(90) Pappenfus, T. M.; Chesterfield, R. J.; Frisbie, C. D.; Mann, K. R.; Casado, J.; Raff, J. D.; Miller, L. L. A π-Stacking Terthiophene-Based Quinodimethane Is an n-Channel Conductor in a Thin Film Transistor. *Journal of the American Chemical Society* **2002**, *124* (16), 4184-4185. DOI: 10.1021/ja025553j.

(91) Chesterfield, R. J.; Newman, C. R.; Pappenfus, T. M.; Ewbank, P. C.; Haukaas, M. H.; Mann, K. R.; Miller, L. L.; Frisbie, C. D. High Electron Mobility and Ambipolar Transport in Organic Thin-Film Transistors Based on a π-Stacking Quinoidal Terthiophene. *Advanced Materials* **2003**, *15* (15), 1278-1282. DOI: https://doi.org/10.1002/adma.200305200.

(92) Gao, X.; Hu, Y. Development of n-type organic semiconductors for thin film transistors: a viewpoint of molecular design. *Journal of Materials Chemistry C* **2014**, *2* (17), 3099-3117, 10.1039/C3TC32046D. DOI: 10.1039/C3TC32046D.

(93) Tsukamoto, K.; Takagi, K.; Nagano, S.; Hara, M.; Ie, Y.; Osakada, K.; Takeuchi, D. π-Extension of electron-accepting dithiarubicene with a cyano-substituted electron-withdrawing group and application in air-stable n-channel organic field effect transistors. *Journal of Materials Chemistry C* **2019**, *7* (40), 12610-12618, 10.1039/C9TC04325J. DOI: 10.1039/C9TC04325J.

(94) Ren, L.; Yuan, D.; Zhu, X. Design of a Quinoidal Thieno[3,4-b]thiophene-Diketopyrrolopyrrole-Based Small Molecule as n-Type Semiconductor. *Chemistry – An Asian Journal* **2019**, *14* (10), 1717-1722. DOI: https://doi.org/10.1002/asia.201801737.

(95) Yamamoto, K.; Kato, S.-i.; Zajaczkowska, H.; Marszalek, T.; Blom, P. W. M.; Ie, Y. Effects of fluorine substitution in quinoidal oligothiophenes for use as organic semiconductors. *Journal of Materials Chemistry C* **2020**, *8* (10), 3580-3588, 10.1039/C9TC06598A. DOI: 10.1039/C9TC06598A.

(96) Lin, Z.; Chen, L.; Xu, Q.; Shao, G.; Zeng, Z.; Wu, D.; Xia, J. Tuning Biradical Character to Enable High and Balanced Ambipolar Charge Transport in a Quinoidal π-System. *Organic Letters* **2020**, *22* (7), 2553-2558. DOI: 10.1021/acs.orglett.0c00453.

(97) Huang, J.; Lu, S.; Chen, P.-A.; Wang, K.; Hu, Y.; Liang, Y.; Wang, M.; Reichmanis, E. Rational Design of a Narrow-Bandgap Conjugated Polymer Using the Quinoidal Thieno[3,2-b]thiophene-Based Building Block for Organic Field-Effect Transistor Applications. *Macromolecules* **2019**, *52* (12), 4749-4756. DOI: 10.1021/acs.macromol.9b00370.

(98) Kim, Y.; Kim, Y.-J.; Kim, Y.-A.; Jung, E.; Mok, Y.; Kim, K.; Hwang, H.; Park, J.-J.; Kim, M.-G.; Mathur, S.; et al. Open-Shell and Closed-Shell Quinoid–Aromatic Conjugated Polymers: Unusual Spin Magnetic and High Charge Transport Properties. *ACS Applied Materials & Interfaces* **2021**, *13* (2), 2887-2898. DOI: 10.1021/acsami.0c15893.

(99) Hwang, H.; Kim, Y.; Kang, M.; Lee, M.-H.; Heo, Y.-J.; Kim, D.-Y. A conjugated polymer with high planarity and extended π-electron delocalization via a quinoid structure prepared by short synthetic steps. *Polymer Chemistry* **2017**, *8* (2), 361-365, 10.1039/C6PY01729K. DOI: 10.1039/C6PY01729K.

(100) Kim, Y.; Yang, D.; Kim, Y.-J.; Jung, E.; Park, J.-J.; Choi, Y.; Kim, Y.; Mathur, S.; Kim, D.-Y. Azaquinoid-Based High Spin Open-Shell Conjugated Polymer for n-Type Organic Field-Effect Transistors. *Advanced Materials Interfaces n/a* (n/a), 2201205. DOI: https://doi.org/10.1002/admi.202201205.

(101) Zhu, Z.; Wang, L.; Gao, C. Chapter 3 - Thermoelectric properties of PEDOTs. In *Advanced PEDOT Thermoelectric Materials*, Jiang, F., Liu, C., Xu, J. Eds.; Woodhead Publishing, 2022; pp 73-95.

(102) Lu, Y.; Yu, Z.-D.; Un, H.-I.; Yao, Z.-F.; You, H.-Y.; Jin, W.; Li, L.; Wang, Z.-Y.; Dong, B.-W.; Barlow, S.; et al. Persistent Conjugated Backbone and Disordered Lamellar Packing Impart Polymers with Efficient n-Doping and High Conductivities. *Advanced Materials* **2021**, *33* (2), 2005946. DOI: https://doi.org/10.1002/adma.202005946.

(103) Sun, Y.; Di, C. A.; Xu, W.; Zhu, D. B. Advances in n-Type Organic Thermoelectric Materials and Devices. *Advanced Electronic Materials* **2019**, *5* (11). DOI: 10.1002/aelm.201800825.

(104) Tripathi, A.; Lee, Y.; Lee, S.; Woo, H. Y. Recent advances in n-type organic thermoelectric materials, dopants, and doping strategies. *Journal of Materials Chemistry C* **2022**, *10* (16), 6114-6140, 10.1039/D1TC06175E. DOI: 10.1039/D1TC06175E.

(105) Zhao, X.; Madan, D.; Cheng, Y.; Zhou, J.; Li, H.; Thon, S. M.; Bragg, A. E.; DeCoster, M. E.; Hopkins, P. E.; Katz, H. E. High Conductivity and Electron-Transfer Validation in an n-Type Fluoride-Anion-Doped Polymer for Thermoelectrics in Air. *Advanced Materials* **2017**, *29* (34), 1606928. DOI: https://doi.org/10.1002/adma.201606928.

(106) Yuan, D.; Huang, D.; Rivero, S. M.; Carreras, A.; Zhang, C.; Zou, Y.; Jiao, X.; McNeill, C. R.; Zhu, X.; Di, C.-a.; et al. Cholesteric Aggregation at the Quinoidal-to-Diradical Border Enabled Stable n-Doped Conductor. *Chem* **2019**, *5* (4), 964-976. DOI: https://doi.org/10.1016/j.chempr.2019.02.010.

(107) Yuan, D.; Guo, Y.; Zeng, Y.; Fan, Q.; Wang, J.; Yi, Y.; Zhu, X. Air-Stable n-Type Thermoelectric Materials Enabled by Organic Diradicaloids. *Angewandte Chemie International Edition* **2019**, *58* (15), 4958-4962. DOI: https://doi.org/10.1002/anie.201814544.

(108) Liu, W.; Li, W.; Yao, J.; Zhan, C. Achieving high short-circuit current and fill-factor via increasing quinoidal character on nonfullerene small molecule acceptor. *Chinese Chemical Letters* **2018**, *29* (3), 381-384. DOI: https://doi.org/10.1016/j.cclet.2017.11.018.